THE UNIVERSITY OF MICHIGAN

COLLEGE OF ENGINEERING
Department of Atmospheric and Oceanic Science

Technical Report

NONLINEAR EXCHANGE PROCESSES IN A BAROTROPIC ATMOSPHERE

Einar Egeland

Aksel C. Wiin-Nielsen
Project Director

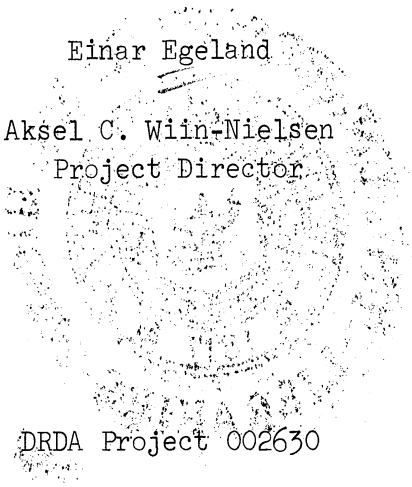

DRDA Project 002630

supported by:

NATIONAL SCIENCE FOUNDATION
GRANT NO. GA-16166
WASHINGTON, D.C.

administered through:

DIVISION OF RESEARCH DEVELOPMENT AND ADMINISTRATION ANN ARBOR

August 1973

enm

UMRC880

TABLE OF CONTENTS

LIST OF ILLUSTRATIONS

LIST OF ILLUSTRATIONS (Concluded)

ABSTRACT

Nonlinear exchange processes of energy and enstrophy between a zonal flow and a disturbance is studied by numerical integrations of a low order set of equations approximating the barotropic vorticity equation, and by numerical integrations of a model which allow for a more general type of flow than what may be described by the low-order system. This last model, called the extended one, uses gridpoints to represent the y-variation of the flow and a spectral representation of the x-direction. Results from numerical integrations of the two models are compared with each other. It is found that the exchange of energy and enstrophy between the zonal flow and the eddies depends on both the shape as well as the wave length of the eddy flow. Both models are tested linearly for stability. By comparing the results from the linear analysis of the different cases with the magnitudes of the two-dimensional wave numbers for the same cases, it is found that the question of stability or instability of the zonal flow is related to how the energy is cascaded when it is given up by the zonal flow.

INTRODUCTION

The purpose of this paper is to investigate nonlinear interactions in a barotropic model atmosphere; with the emphasis on the exchanges of energy and enstrophy between the zonal flow and the eddy flow. Also we shall explore some of the properties of the two atmospheric models that we are going to use for the study of nonlinear interactions.

Probably the most well-known work in the field of nonlinear interactions is the work by Fjørtoft (1953). In this work the so-called blocking theorem for energy flow is derived. Later this work was extended by Charney and Stern (1962) who showed that a similar theorem could be derived for quasi-geostrophic flow provided one made the gradient of the potential temperature vanish at the ground.

The transfer of energy between the mean flow and a disturbance in a barotropic nondivergent fluid has been investigated by Platzman (1952) and by Wiin-Nielsen (1961). In the present paper we shall use the low-order system of equations derived by Wiin-Nielsen in the above paper.

The use of low-order spectral systems was initiated by Lorenz (1960). He also used his maximum simplified system of equations to study the transfer of energy between the zonal flow and a disturbance. The method of using a low-order system of equations to study energy transfer has been used extensively by Baer (1970a, 1970b, 1971).

Diagnostic studies of nonlinear interactions using atmospheric data have been carried out by Yang (1967) and by Steinberg (1971).

One of the purposes of the present report is to provide material which can be used for instructional purposes. It was therefore decided to include a review of some well established results and adapt them to the cases considered here. For the same reason, the mathematical derivations have been given in detail in most cases where it was thought to be necessary.

CHAPTER 1

A SIMPLE EXAMPLE OF NONLINEAR INTERACTIONS

In order to see in a simple way what nonlinear interactions mean, at least mathematically, we shall use the simple equation

$$\frac{\partial u}{\partial t} + u_o \frac{\partial u}{\partial x} = 0 . \tag{1.1}$$

With u_o being a constant this is the linear advection equation. In this context we shall regard u as a function of one space coordinate, x, and time, t. Then at each time step u may be written as the sum of a Fourier series:

$$u = \sum_m \hat{u}_m(t)\, e^{imx} .$$

From this expression we obtain for the derivatives:

$$\frac{\partial u}{\partial t} = \sum_m \frac{d\hat{u}_m}{dt} e^{imx} ,$$

$$\frac{\partial u}{\partial x} = i \sum_m m\hat{u}_m(t)\, e^{imx} .$$

Substituting these expressions for the derivatives in (1.1), we get

$$\sum_m e^{imx} \left\{ \frac{d\hat{u}_m}{dt} + iu_o m\hat{u}_m \right\} = 0 . \tag{1.2}$$

In order to satisfy this equation the following relation must hold for every m

$$\frac{d\hat{u}_m}{dt} + iu_o m\hat{u}_m = 0 . \tag{1.3}$$

Thus we have obtained an equation for each of the time dependent amplitudes. The set of equations (1.3) is called the spectral form of the equation (1.1).

If, on the other hand, we allow u_o to become time and space dependent, as it will be in the meteorological equations, we get an expression for $d\hat{u}_m/dt$

which is somewhat different from (1.3). Making $u_o = u$ in (1.1) we get the non-linear advection equation

$$\frac{\partial u}{\partial t} + u \frac{\partial u}{\partial x} = 0 . \tag{1.4}$$

An extensive amount of work has been carried out in order to obtain analytic solutions of (1.4) and equations related to it. One contribution to these investigations was given by G. Platzman in 1964 (Platzman, 1964). In this work he points out that even for the more general equation

$$\frac{\partial u}{\partial t} + u \frac{\partial u}{\partial x} = \nu \frac{\partial^2 u}{\partial x^2} ,$$

one may obtain an exact, general solution. Also he remarks that "—the nonlinear term $u(\partial u/\partial x)$ contains the most rudimentary form of the mechanism whereby the spectrum of motion is modified through inertial exchange between spectral components of different scales." This interaction of all the different scales may be showed mathematically if we substitute the spectral expressions for both u and its derivatives into (1.4). Doing this we get:

$$\sum_m \frac{d\hat{u}_m}{dt} e^{imx} + i \sum_{p'} \hat{u}_{p'}(t) e^{ip'x} \sum_p p\hat{u}_p(t) e^{ipx} = 0 , \tag{1.5}$$

p and p' are, like m, wave numbers in the x-direction. In order to simplify the equation above we put $p + p' = m$. Assuming this relation (1.5) may be written:

$$\sum_m e^{imx} \left\{ \frac{d\hat{u}_m}{dt} + i \sum_{p'} p\hat{u}_{p'}(t)\hat{u}_p(t) \right\} = 0 , \qquad p' = m-p . \tag{1.5a}$$

In order to satisfy (1.5a) we must have for every m

$$\frac{d\hat{u}_m}{dt} + i \sum_p \hat{u}_{p'}(t)\hat{u}_p(t) = 0 , \qquad p' = m-p . \tag{1.6}$$

From this equation we see that when u_o is no longer a constant, but becomes time and space dependent, the change of $\hat{u}_m$ is no longer determined by the amplitude of that wave number alone, but it depends on the sum of the products $\hat{u}_{p'}\hat{u}_p$. In other words, the change of the amplitude on one scale is no longer independent of the other scales as in the linear case, but is given by a sum of covariances expressing the interactions between the different scales.

CHAPTER 2

CONSERVATION OF ENERGY AND ENSTROPHY AND RESTRICTIONS ON THE EXCHANGE OF ENERGY

In this chapter we will show that both total energy and total enstrophy (mean squared vorticity) are conserved for the case of barotropic flow, provided certain boundary conditions are fulfilled. For this type of flow the governing equation is the barotropic vorticity equation

$$\frac{\partial \zeta}{\partial t} + \vec{v} \cdot \nabla(f+\zeta) = 0 . \tag{2.1}$$

Assuming that the velocity, $\vec{v}$, is nondivergent, it may be expressed in terms of a streamfunction, ψ:

$$\vec{v} = \vec{k} \times \nabla\psi .$$

The vorticity, ζ, now may be written

$$\zeta = \nabla^2\psi .$$

Using these expressions we get an equation with one dependent variable, ψ:

$$\frac{\partial}{\partial t}\nabla^2\psi + \vec{k} \cdot \{\nabla\psi \times \nabla\nabla^2\psi\} + \beta \frac{\partial \psi}{\partial x} = 0 . \tag{2.2}$$

Before going any further we will assume that the motion is taking place in a β-plane channel bounded to the north and south by rigid walls. Moreover, the flow will be assumed to be periodic in the east-west direction. With D being the width of the channel and L_x the wave length in the zonal direction, the total kinetic energy per unit area is

$$\bar{K} = \frac{1}{L_x D} \int_0^{L_x} \int_0^{D} \frac{\vec{v}\cdot\vec{v}}{2} \, dy dx . \tag{2.3}$$

Using the streamfunction (2.3) becomes

$$\bar{K} = \frac{1}{2L_x D} \int_0^{L_x} \int_0^{D} \nabla\psi \cdot \nabla\psi \, dydx . \qquad (2.3a)$$

The time rate of change of $\bar{K}$ is

$$\frac{d\bar{K}}{dt} = \frac{1}{L_x D} \int_0^{L_x} \int_0^{D} \nabla\psi \cdot \nabla \frac{\partial\psi}{\partial t} \, dydx = -\frac{1}{L_x D} \int_0^{L_x} \int_0^{D} \psi\nabla^2 \frac{\partial\psi}{\partial t} \, dydx .$$

The last integral has been obtained by using the identity

$$\nabla \cdot \left(\psi\nabla \frac{\partial\psi}{\partial t}\right) = \nabla\psi \cdot \nabla \frac{\partial\psi}{\partial t} + \psi\nabla^2 \frac{\partial\psi}{\partial t} .$$

Integrating the term on the left, we get

$$\int_0^{L_x} \int_0^{D} \nabla \cdot \left(\psi\nabla \frac{\partial\psi}{\partial t}\right) dydx = \oint_C \delta\vec{r} \times \vec{k} \cdot \left(\psi\nabla \frac{\partial\psi}{\partial t}\right) .$$

C means the total circumference of the area we are integrating over, $\delta\vec{r}$ is a vector line element being tangential to the circumference. From this line integral we see that the integral on the left vanishes if, in addition to the boundary conditions we have already, we also demand that $\partial\psi/\partial t \equiv 0$ along the northern and southern boundaries. The condition of periodicity will make the contributions from the western and eastern boundaries cancel each other. Having made the assumption $\partial\psi/\partial t \equiv 0$ at $y = 0$ and $y = D$ we now proceed to evaluate the integral

$$-\frac{1}{L_x D} \int_0^{L_x} \int_0^{D} \psi\nabla^2 \frac{\partial\psi}{\partial t} \, dydx .$$

Using the equation of motion (2.1) this integral becomes

$$\frac{1}{L_x D} \int_0^{L_x} \int_0^{D} \psi\{\vec{v} \cdot \nabla(f+\zeta)\} dydx = \frac{1}{L_x D} \int_0^{L_x} \int_0^{D} \psi\nabla \cdot (\vec{v}\zeta) dydx +$$

$$+ \frac{1}{L_x D} \int_0^{L_x} \int_0^{D} \psi \frac{\partial\psi}{\partial x} \beta \, dydx =$$

$$= \frac{1}{L_x D} \int_0^{L_x} \int_0^{D} \nabla \cdot (\vec{v}\psi\zeta) dydx - \frac{1}{L_x D} \int_0^{L_x} \int_0^{D} \zeta(\vec{k} \times \nabla\psi) \cdot \nabla\psi \, dydx + \frac{\beta}{L_x D} \int_0^{D} \int_0^{L_x} \frac{\partial}{\partial x} \psi^2 \, dxdy .$$

The first integral above may be transformed into

$$\frac{1}{L_x D} \oint_C \delta\vec{r} \times \vec{k} \cdot (\vec{v}\psi\zeta) .$$

Along the northern and southern boundaries $(\delta\vec{r} \times \vec{k}) \cdot \vec{v} = 0$ at all points. Hence, we get no contributions to the integral from here. Along the eastern and western boundaries the contributions cancel in pairs because of the periodicity condition. The second integral above is zero because

$$(\vec{k} \times \nabla\psi) \cdot \nabla\psi \equiv 0 .$$

Finally, the third integral is zero because of the periodicity condition. Hence, we conclude that:

$$\frac{d\bar{K}}{dt} = 0 \tag{2.4}$$

The mean squared voriticity is defined by

$$\bar{V} = \frac{1}{L_x D} \int_0^{L_x} \int_0^{D} \frac{(\nabla^2\psi)^2}{2} \, dydx . \tag{2.5}$$

By a procedure similar to the one used to obtain (2.4) one may show that

$$\frac{d\bar{V}}{dt} = 0 . \tag{2.6}$$

Hence, for the type of flow we are studying both total kinetic energy and total enstrophy is conserved.

Next we want to show that the exchange of energy between the different scales of the motion is restricted. This was first done by Fjørtoft (1953). His analysis was based on barotropic motion on a sphere. Below we will repeat parts of this work using a β-plane geometry instead of a sphere. In order to separate the energy and enstrophy into their components on each scale of the motion, we write the streamfunction

$$\psi(x,y,t) = \sum_m \sum_n \hat{\psi}_{mn}(t) \, e^{i(mx + ny)} . \tag{2.7}$$

$\sum_m \sum_n$ means that we sum over all wave numbers in the x-, and in the y-direction that we want to include in our model. For all practical purposes the number of waves included will, of course, be finite.

Using the expression (2.7) for the streamfield we find that (2.3a) and (2.5) may be written:

$$\bar{K} = \frac{1}{2} \sum_m \sum_n \hat{\psi}^2_{mn} (m^2+n^2) , \tag{2.8}$$

$$\bar{V} = \frac{1}{2} \sum_m \sum_n \hat{\psi}^2_{mn} (m^2+n^2)^2 , \tag{2.9}$$

provided we are able to satisfy simultaneously the boundary conditions that we have imposed on the flow and the conditions of periodicity which are required in order to arrive at (2.8) and (2.9). For the zonal direction there is no problem because we assume that the flow is periodic in this direction. One way to assure that the normal velocity vanishes at every point along the southern and northern boundaries is to make an expansion in only sine functions in the y-direction and to restrict n to be integer multiples of π/D. With this assumption the streamfunction is identically zero at all times along the southern and northern boundaries. Moreover ψ is periodic with a wavelength 2D in the y-direction, but because we express it by sine functions only these functions are orthogonal on the interval $0 \leq y \leq D$. Hence, we know that ψ may be written in terms of functions which are orthogonal on the area we are integrating over. This is what we need to form (2.8) and (2.9).

If we introduce the two-dimensional wave number $q^2 = m^2 + n^2$ we may write (2.8) and (2.9) in the following way

$$\bar{K} = \frac{1}{2} \sum_q \sum_m \hat{\psi}^2_{mn} \, q^2 = \frac{1}{2} \sum_q \sum_m \hat{\psi}^2_{mn} \, q^2 = \sum_q K_q , \tag{2.8a}$$

$$\bar{V} = \frac{1}{2} \sum_q \sum_m \hat{\psi}^2_{mn} \, q^4 = \frac{1}{2} \sum_q q^2 \sum_m \hat{\psi}^2_{mn} \, q^2 = \sum_q q^2 \, K_q . \tag{2.9a}$$

Here

$$K_q = \frac{1}{2} q^2 \sum_m \hat{\psi}^2_{mn} , \qquad n^2 = q^2 - m^2 .$$

K_q is the kinetic energy associated with the total wave number q. When we sum over m we include only those $\hat{\psi}^2_{mn}$ for which n satisfies the relation $n^2 = q^2 - m^2$. Depending on the relation between L_x and D there will be one or more terms in this sum for each value of q.

We may now make the following mechanical interpretation of the conditions $\bar{K}$ = const. and $\bar{V}$ = const. This mechanical analogue of what we now call "Fjørtoft's blocking theorem" was first invented by Charney (1966). Imagine that we have a weightless rod on which we suspend weights: $K_1, K_2, \ldots$, etc., at the distances $q_1^2, q_2^2, \ldots$, etc. (Figure 2.1), and that these weights are balanced by $\bar{V}$. Equation (2.9) may also be written

$$\sum_q q^2 K_q - l \cdot \bar{V} = 0, \tag{2.10}$$

expressing the fact that the system we have made is in mechanical equilibrium at any time. From our conservation theorems (2.4) and (2.6) together with (2.10) we may now deduce that the total mass of the weights is the same at any time, moreover these weights must always be arranged in such a way that the system is kept in equilibrium.

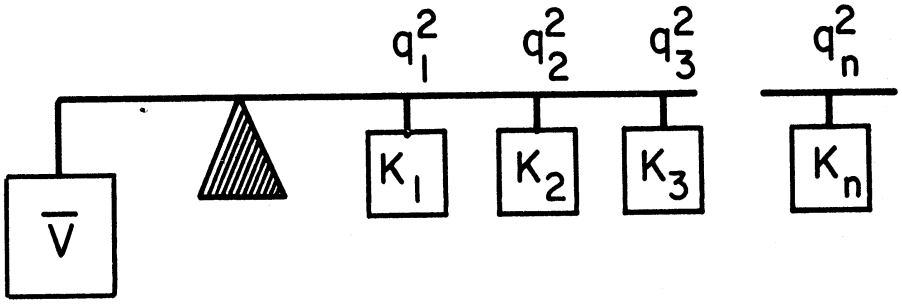

Figure 2.1. Mechanical interpretation of the equation $\sum_q q^2 K_q - l \cdot \bar{V} = 0$.

Returning back to the atmosphere we shall see how the energy exchange between the different parts of the flow becomes restricted because of the conservation of energy and enstrophy. We will assume that there is an exchange of energy going on between parts of the flow having total wave numbers q_1, q_2, and q_3. Also we will assume that $q_1^2 < q_3^2$. For this simple system the conservation of energy and enstrophy may be written

$$\begin{aligned} \Delta K_{q_1} + \Delta K_{q_2} + \Delta K_{q_3} &= 0, \\ q_1^2 \Delta K_{q_1} + q_2^2 \Delta K_{q_2} + q_3^2 \Delta K_{q_3} &= 0. \end{aligned} \tag{2.11}$$

Δ means the difference between the kinetic energy associated with a certain wave number at the present time and a previous time. The system of equations (2.11) may be solved for two ΔK's in terms of the third one. Solving for ΔK_{q_1} and ΔK_{q_3} we get:

$$\Delta K_{q_1} = -\frac{q_3^2 - q_2^2}{q_3^2 - q_1^2}\,\Delta K_{q_2},$$

$$\Delta K_{q_3} = -\frac{q_2^2 - q_1^2}{q_3^2 - q_1^2}\,\Delta K_{q_2}.$$

Based on these solutions one may ask: Under what conditions will ΔK_{q_1} and ΔK_{q_3} have a sign opposite to the sign of ΔK_{q_2}? For this to occur we must have

$$\frac{q_3^2 - q_2^2}{q_3^2 - q_1^2} > 0, \quad \text{and} \quad \frac{q_2^2 - q_1^2}{q_3^2 - q_1^2} > 0,$$

simultaneously. In order to satisfy both inequalities we must have

$$q_1^2 < q_2^2 < q_3^2.$$

From this we conclude that no part of the flow can be a source or a sink of energy unless it is at an intermediate scale. Hence, energy cannot flow consistently in one direction. Any flow of energy from smaller to larger scales must be balanced by flow in the opposite direction.

CHAPTER 3

DERIVATION OF THE EQUATIONS FOR TWO LOW-ORDER SYSTEMS

In this chapter we will derive two different sets of equations which may be used for the numerical integration of the barotropic vorticity equation. The first set of equations will approximate the barotropic vorticity equation in a very crude way. The second set will be more general, and hence, a better approximation.

The first set of equations are derived following the analysis given by Wiin-Nielsen (1961). In this case we restrict the zonal flow to be of the form:

$$\bar{u}(y,t) = B(t) + C(t) - B(t)\cos(2\lambda y) - C(t)\cos(4\lambda y). \qquad (3.1)$$

The family of curves described by this function for given values B and C can vary between strong westerlies in the center of the channel with easterlies near the walls and, on the other extreme, strong westerlies near the walls with easterlies in the center of the channel. The streamfunction corresponding to (3.1) is:

$$\bar{\psi}(y,t) = D(B+C)\left[1 - \frac{y}{D}\right] + \frac{B}{2\lambda}\sin(2\lambda y) + \frac{C}{4\lambda}\sin(4\lambda y). \qquad (3.2)$$

For the perturbation flow we will use a streamfield of the form:

$$\psi'(x,y,t) = \frac{E_1(t)}{k}\sin(\lambda y)\sin(kx) + \frac{E_3(t)}{k}\sin(3\lambda y)\sin(kx) + \frac{F_1(t)}{k}\sin(\lambda y)\cos(kx) + \frac{F_3(t)}{k}\sin(3\lambda y)\cos(kx), \qquad (3.3)$$

which allows for one wave number (k) in the zonal direction and two wave numbers (λ and 3λ) in the meridional direction. The complete streamfunction is then given by the expression

$$\psi(x,y,t) = \bar{\psi}(y,t) + \psi'(x,y,t). \qquad (3.4)$$

Note that the boundary conditions that we had to choose in order to get conservation of energy and enstrophy are satisfied when we define our streamfield

by (4.2) and (4.3). Equation (3.4) may now be substituted into the vorticity equation (2.1). By using the technique developed by Lorenz (1960) we get six forecast equations for the six amplitudes: B, C, E_1, E_3, F_1, F_3. These six equations will be a coupled set of ordinary differential equations because the amplitudes are functions of time only. With the notations

$$Q = \frac{\lambda^2}{k^2}, \qquad R = \frac{\beta}{k^2},$$

the set of equations is

$$\frac{dB}{dt} = 2kQ[E_1F_3 - E_3F_1],$$

$$\frac{dC}{dt} = -2kQ[E_1F_3 - E_3F_1],$$

$$\frac{dE_1}{dt} = k\left[CF_1 - \frac{Q-3}{2(Q+1)}BF_1 - \frac{5Q+1}{2(Q+1)}BF_3 - \frac{7Q-1}{2(Q+1)}CF_3 - \frac{R}{Q+1}F_1\right],$$

$$\frac{dE_3}{dt} = k\left[(B+C)F_3 + \frac{3Q-1}{2(9Q+1)}BF_1 - \frac{15Q-1}{2(9Q+1)}CF_1 - \frac{R}{9Q+1}F_3\right],$$

$$\frac{dF_1}{dt} = -k\left[CE_1 - \frac{Q-3}{2(Q+1)}BE_1 - \frac{5Q+1}{2(Q+1)}BE_3 - \frac{7Q-1}{2(Q+1)}CE_3 - \frac{R}{Q+1}E_1\right],$$

$$\frac{dF_3}{dt} = -k\left[(B+C)E_3 + \frac{3Q-1}{2(9Q+1)}BE_1 - \frac{15Q-1}{2(9Q+1)}CE_1 - \frac{R}{9Q+1}E_3\right], \qquad (3.5)$$

We notice from the first two expressions in (3.5) that

$$\frac{d}{dt}(B+C) = 0 \qquad (3.6)$$

Hence the changes in time of B and C are not independent of each other. Physically (3.6) expresses that the total zonal momentum of the system is conserved.

From the streamfield (3.2) and (3.3) we see that our system of equations (3.5) describes the changes in a barotropic flow which contains the spectral components 0 and 1 in the zonal direction and 0, 1, 2, 3, and 4 in the latitudinal direction. Hence, any flow pattern that we get by integrating (3.5) is made up of these spectral components.

We will next show how one may derive a system of equations which describes the changes with time of a flow having the same two components in the zonal

direction, but which is completely arbitrary in the south-north direction. I.e., which has infinitely many spectral components in this direction. However, the values of the dependent variables have to be calculated using gridpoints in the north-south direction. This then puts a practical limit to the number of degrees of freedom that we can allow the model to have.

The set of equations for this model is obtained in the following way: We start from a streamfield of the form

$$\psi(x,y,t) = A_1(y,t) + A_2(y,t)\cos kx + A_3(y,t)\sin kx . \qquad (3.7)$$

This then gives the following expression for the vorticity:

$$\zeta = \frac{\partial^2 A_1}{\partial y^2} + \left(\frac{\partial^2 A_2}{\partial y^2} - k^2 A_2\right)\cos kx + \left(\frac{\partial^2 A_3}{\partial y^2} - k^2 A_3\right)\sin kx . \qquad (3.8)$$

From these two expressions we calculate $\partial\zeta/dt$, $-\beta(\partial\psi/\partial x)$, and $-\vec{k}\cdot(\nabla\psi x\nabla\zeta)$. This gives us an expression for each term in the vorticity equation. Combining them all together we find that in order to satisfy the vorticity equation we must have

$$\begin{aligned}
\frac{\partial}{\partial t}\left(\frac{\partial^2 A_1}{\partial y^2}\right) &= \frac{k}{2}\frac{\partial}{\partial y}\left[A_2\left(\frac{\partial^2 A_3}{\partial y^2} - k^2 A_3\right) - A_3\left(\frac{\partial^2 A_2}{\partial y^2} - k^2 A_2\right)\right], \\
\frac{\partial}{\partial t}\left(\frac{\partial^2 A_2}{\partial y^2} - k^2 A_2\right) &= k\left[\left(\frac{\partial^2 A_3}{\partial y^2} - k^2 A_3\right)\frac{\partial A_1}{\partial y} - A_3\left(\frac{\partial^3 A_1}{\partial y^3}\right)\right] - \beta k A_3 , \\
\frac{\partial}{\partial t}\left(\frac{\partial^2 A_3}{\partial y^2} - k^2 A_3\right) &= -k\left[\left(\frac{\partial^2 A_2}{\partial y^2} - k^2 A_2\right)\frac{\partial A_1}{\partial y} - A_2\left(\frac{\partial^3 A_1}{\partial y^3}\right)\right] + \beta k A_2 ,
\end{aligned} \qquad (3.9)$$

The velocity of the mean flow is given by $\bar{u} = -(\partial A_1/\partial y)$. We will now integrate the first equation above, writing $\bar{u}$ instead of $-(\partial A_1/\partial y)$, and using the boundary conditions

$$\begin{aligned}
\frac{\partial \bar{u}}{\partial t} &= 0 \quad \text{at} \quad y = 0 , \\
A_2 &= 0 \quad \text{at} \quad y = 0 , \\
A_3 &= 0 \quad \text{at} \quad y = 0 ,
\end{aligned} \qquad (3.10)$$

we get

$$\frac{\partial \bar{u}}{\partial t} = -\frac{k}{2}\left[A_2 \frac{\partial^2 A_3}{\partial y^2} - A_3 \frac{\partial^2 A_3}{\partial y^2}\right], \tag{3.11}$$

From the relation

$$A_2 \frac{\partial^2 A_3}{\partial y^2} - A_3 \frac{\partial^2 A_2}{\partial y^2} = \frac{\partial}{\partial y}\left[A_2 \frac{\partial A_3}{\partial y} - A_3 \frac{\partial A_2}{\partial y}\right],$$

we see that this equation may finally be written

$$\frac{\partial \bar{u}}{\partial t} = -\frac{k}{2}\frac{\partial}{\partial y}\left[A_2 \frac{\partial A_3}{\partial y} - A_3 \frac{\partial A_2}{\partial y}\right]. \tag{3.11a}$$

Next we define

$$V_s = kA_2,$$

$$V_c = kA_3, \tag{3.12}$$

and

$$W_s = \frac{\partial^2 V_s}{\partial y^2} - k^2 V_s,$$

$$W_c = \frac{\partial^2 V_c}{\partial y^2} - k^2 V_c. \tag{3.13}$$

If (3.12) and (3.13) is now substituted into (3.11a) and the last two equations of (3.9), we get these three equations written in the form

$$\frac{\partial \bar{u}}{\partial t} = -\frac{1}{2k}\left[V_s \frac{\partial^2 V_c}{\partial y^2} - V_c \frac{\partial^2 V_s}{\partial y^2}\right],$$

$$\frac{\partial W_s}{\partial t} = -k\bar{u}W_c - k\left(\beta - \frac{\partial^2 \bar{u}}{\partial y^2}\right)V_c,$$

$$\frac{\partial W_c}{\partial t} = k\bar{u}W_s + k\left(\beta - \frac{\partial^2 \bar{u}}{\partial y^2}\right)V_s, \tag{3.14}$$

When (3.14) is integrated numerically we also have to include (3.13) in our set of equations. This is because we compute only the time changes of $\bar{u}$, W_s, and W_c from (3.14), but on the other hand the values of V_s and V_c are necessary in order to compute the time derivatives in (3.14). Hence, at each time step we must solve the equations

$$\frac{\partial^2 V_s}{\partial y^2} - k^2 V_s = W_s ,$$

$$\frac{\partial^2 V_c}{\partial y^2} - k^2 V_c = W_c , \qquad (3.13a)$$

for V_s and V_c regarding W_s and W_c as known quantities.

The numerical integration of this model will be carried out with the following set of boundary conditions

$$\bar{u} = 0 \quad \text{at} \quad y = 0 \quad \text{and} \quad y = D ,$$

$$V_c = 0 \quad \text{at} \quad y = 0 \quad \text{and} \quad y = D ,$$

$$V_s = 0 \quad \text{at} \quad y = 0 \quad \text{and} \quad y = D . \qquad (3.15)$$

CHAPTER 4

ENERGETICS OF THE MODELS

When we derived the equations governing the motions in the very simple model we made a distinction between the zonal flow, or mean flow, and the x-dependent part of the flow. This distinction came about when we specified the streamfunctions of the zonal flow and the x-dependent flow separately. Hence, the amplitudes B and C are related to the zonal flow while E_1, E_3, F_1, and F_3 are related to the x-dependent part of the flow or, as it is also being called, the eddy flow. Because all these amplitudes are calculated separately we are able to see how both parts of the flow change during the integration and how they influence each other.

For the second model we made no explicit statement regarding these two separate parts of the flow (zonal flow and eddy flow). However, as one may see, part of the streamfunction does not depend on x. This then is the part of the streamfunction which describes the zonal flow. Moreover, in this model we have the magnitude of the zonal flow as a dependent variable. Hence, here too we are able to follow the changes in the two parts of the flow separately and also to see how they interact. Studying the nonlinear interactions between the zonal flow and the eddies is one way of obtaining information about the dynamics of the model. Because of that this chapter will be devoted to the derivation of some energy formulae that we need for this study. In Chapter 6 we will investigate the dynamic stability of the flow. Here too, the distinction between the zonal flow and the eddies will be essential.

To obtain the desired energy formulae we want we start with (2.2) which may be written

$$\frac{\partial \zeta}{\partial t} + \vec{v} \cdot \nabla \zeta + \beta \frac{\partial \psi}{\partial x} = 0 . \tag{4.1}$$

Each of the quantities in this equation will now be separated into a zonal mean value and the deviation from this mean value.

$$\zeta = \bar{\zeta} + \zeta' ,$$

$$\vec{v} = \bar{\vec{v}} + \vec{v}' ,$$

$$\psi = \bar{\psi} + \psi' .$$

By definition then $\bar{\zeta} = \bar{\vec{v}}' = \bar{\psi}' = 0$, and $\partial\bar{\zeta}/\partial x = \partial\bar{\vec{v}}/\partial x = \partial\bar{\psi}/\partial x = 0$. If we put $\nabla\psi = \nabla\bar{\psi} + \nabla\psi'$ in (2.3a) this formula becomes

$$\bar{K} = \frac{1}{2D}\int_0^D \nabla\bar{\psi}\cdot\nabla\bar{\psi}\,dy + \frac{1}{2L_x D}\int_0^D\int_0^{L_x} \nabla\psi'\cdot\nabla\psi'\,dxdy = K_z + K_s .$$

This separates the total kinetic energy into the kinetic energy of the zonal flow and the kinetic energy of the eddy flow. Using the separation indicated above (4.1) becomes

$$\frac{\partial\bar{\zeta}}{\partial t} + \frac{\partial\zeta'}{\partial t} + (\bar{\vec{v}} + \vec{v}')\cdot(\nabla\bar{\zeta} + \nabla\zeta') + \beta\frac{\partial\psi'}{\partial x} = 0 ,$$

$$\frac{\partial\bar{\zeta}}{\partial t} + \frac{\partial\zeta'}{\partial t} + \bar{u}\frac{\partial\bar{\zeta}}{\partial x} + \bar{u}\frac{\partial\zeta'}{\partial x} + \frac{\partial\psi'}{\partial x}\frac{\partial\bar{\zeta}}{\partial y} + \vec{v}'\cdot\nabla\zeta' + \beta\frac{\partial\psi'}{\partial x} = 0 .$$

The term $\bar{u}(\partial\bar{\zeta}/\partial x) = 0$ because $\bar{\zeta}$ is not a function of x. If we take the zonal mean of the last equation, we get:

$$\frac{\partial\bar{\zeta}}{\partial t} + \overline{\vec{v}'\cdot\nabla\zeta'} = 0 . \qquad (4.2)$$

Using the fact that the wind is nondivergent $\overline{\vec{v}'\cdot\nabla\zeta'}$ may be written

$$\overline{\vec{v}'\cdot\nabla\zeta'} = \overline{\nabla\cdot(\zeta'\vec{v})} = \frac{\partial}{\partial y}\overline{(\zeta'v')} = -\frac{\partial}{\partial y}\overline{\left(v'\frac{\partial u'}{\partial y}\right)} ,$$

or, by the derivative of a product

$$-\frac{\partial}{\partial y}\overline{\left(v'\frac{\partial u'}{\partial y}\right)} = -\frac{\partial^2}{\partial y^2}\overline{(u'v')} + \frac{\partial}{\partial y}\overline{\left(u'\frac{\partial v'}{\partial y}\right)} .$$

The continuity equation is $\partial u'/\partial x + \partial v'/\partial y = 0$. Multiplication of this by u' gives

$$\frac{1}{2}\frac{\partial}{\partial x}(u')^2 + u'\frac{\partial v'}{\partial y} = 0$$

Finally, by taking the zonal mean of this equation we get

$$\overline{u' \frac{\partial v'}{\partial y}} = 0 .$$

Hence, equation (4.2) may be written

$$\frac{\partial \bar{\zeta}}{\partial t} = \frac{\partial^2}{\partial y^2} \overline{(u'v')} . \tag{4.2a}$$

In the second chapter we obtained the formula

$$\frac{d\bar{K}}{dt} = - \frac{1}{L_x D} \int_0^{L_x} \int_0^{D} \psi \nabla^2 \frac{\partial \psi}{\partial t} \, dy dx .$$

If in this formulae, too, we separate the streamfunction into its zonal mean and the deviation from this mean value and get

$$\frac{d\bar{K}}{dt} = - \frac{1}{L_x D} \int_0^{L_x} \int_0^{D} \bar{\psi} \frac{\partial \bar{\zeta}}{\partial t} \, dy dx - \frac{1}{L_x D} \int_0^{L_x} \int_0^{D} \psi' \frac{\partial \zeta'}{\partial t} \, dy dx . \tag{4.3}$$

From Chapter 2 we know that $d\bar{K}/dt = 0$. The first integral on the right-hand side evidently represents the change in time of the zonal kinetic energy and the second one the change with time of the eddy kinetic energy. Because the total kinetic energy is conserved, these changes have to be equal in magnitude but opposite in signs. Hence, a formula for the conversion of eddy kinetic energy into zonal kinetic energy or vice versa may be obtained from either one of these integrals. Taking the first one, we get

$$\frac{dK_Z}{dt} = - \frac{1}{D} \int_0^{D} \bar{\psi} \frac{\partial \bar{\zeta}}{\partial t} \, dy .$$

Using (4.2) this becomes

$$\frac{dK_Z}{dt} = - \frac{1}{D} \int_0^{D} \bar{\psi} \frac{\partial^2 \overline{(u'v')}}{\partial y^2} \, dy = - \frac{1}{D} \int_0^{D} \bar{u} \frac{\partial \overline{(u'v')}}{\partial y} \, dy .$$

If we had started from the second integral of (4.3) we would have obtained

$$\frac{dK_E}{dt} = \frac{1}{D} \int_0^{D} \bar{u} \frac{\partial \overline{(u'v')}}{\partial y} \, dy .$$

From these results we see that the conversion of zonal kinetic energy into eddy kinetic energy is given by

$$\{K_Z, K_E\} = \frac{1}{D}\int_0^D \bar{u}\,\frac{\partial\overline{(u'v')}}{\partial y}\,dy\,. \qquad (4.4)$$

This expression tells us that if the zonal wind is positively correlated with the convergence of momentum transport there is a conversion from eddy kinetic energy to the mean flow kinetic energy, while negative correlations between these two quantities give rise to the opposite conversion.

The zonal velocity is $\bar{u} = -(\partial\bar{\psi}/\partial y)$ ($\bar{v} = (\partial/\partial x)\psi \equiv 0$. We will now show that under the boundary condition $\partial\psi/\partial t \equiv 0$ at $y = 0$ and at $y = D$ the mean value of $\bar{u}$, calculated in the y-direction, is time independent. This mean value is given by

$$\bar{u}_M = \frac{1}{D}\int_0^D \bar{u}\,dy = -\frac{1}{D}\int_0^D \frac{\partial\bar{\psi}}{\partial y}\,dy = -\frac{1}{D}\{\bar{\psi}_D - \bar{\psi}_0\},$$

Which shows that $\bar{u}_M$ is independent of time because $\bar{\psi}_D$ and $\bar{\psi}_0$ are. This conservation in time of $\bar{u}_M$ implies that only a certain fraction of the zonal kinetic energy may be converted into eddy kinetic energy. The amount available for conversion is found in the following way: Starting with

$$\bar{u} = \bar{u}_M + \bar{u}'\,. \qquad (4.5)$$

The zonal kinetic energy is

$$K_Z = \frac{1}{2D}\int_0^D \bar{u}^2\,dy\,. \qquad (4.6)$$

This equation has also been used by Platzman (1952) in his investigation of the transfer of energy between the mean flow and a disturbance for the same kind of flow as we are dealing with. Using (4.5) we may separate the integrand in (4.6) into two terms

$$K_Z = \frac{1}{2D}\int_0^D (\bar{u}_M + \bar{u}')^2\,dy = \frac{1}{2}\bar{u}_M^2 + \frac{1}{2D}\int_0^D (\bar{u}')^2\,dy\,.$$

The first term on the right-hand side does not change with time, hence this part of the energy cannot be converted into eddy kinetic energy. The available part is given by the second term. Using (4.5) once more this term becomes

$$K_{ZAV} = \frac{1}{2D}\int_0^D (\bar{u} - \bar{u}_M)^2 dy . \tag{4.7}$$

The mean squared vorticity is defined by

$$\bar{V} = \frac{1}{L_x D}\int_0^{L_x}\int_0^D \frac{\zeta^2}{2}\, dydx . \tag{2.5}$$

This, too, may be separated into two parts, one depending only on the zonal flow and another depending on the eddy flow. These parts we will call V_Z and V_E, respectively. We get the expressions for them by writing

$$\zeta = \bar{\zeta} + \zeta' .$$

If this expression is substituted for ζ in the integral above we get

$$\bar{V} = \frac{1}{D}\int_0^D \frac{\bar{\zeta}^2}{2}\, dy + \frac{1}{L_x D}\int_0^{L_x}\int_0^D \frac{(\zeta')^2}{2}\, dydx = V_Z + V_E .$$

The formula giving the conversion of zonal kinetic energy into eddy kinetic energy or vice versa may be obtained by forming dV_Z/dt or dV_E/dt. The simplest seems to be to use dV_Z/dt.

$$\frac{dV_Z}{dt} = \frac{1}{D}\int_0^D \bar{\zeta}\frac{\partial\bar{\zeta}}{\partial t}\, dy .$$

By using (4.2a) and performing an integration by parts we get

$$\frac{dV_Z}{dt} = \frac{1}{D}\int_0^D \frac{\partial^2\bar{u}}{\partial t^2}\frac{\partial\overline{(u'v')}}{\partial y}\, dy \tag{4.8}$$

We see that if the integral is positive we get an increase of zonal enstrophy. This increase must be compensated by an equal decrease of eddy enstrophy. Hence, we may obtain the conversion of zonal enstrophy into eddy enstrophy from the formula

$$\{V_Z, V_E\} = -\frac{1}{D}\int_0^D \frac{\partial^2\bar{u}}{\partial y^2}\cdot\frac{\partial\overline{(u'v')}}{\partial y}\, dy . \tag{4.9}$$

We found above when we worked with the kinetic energy that the boundary condition $\partial\psi/\partial t \equiv 0$ at $y = 0$ and $y = D$ implies that the mean zonal velocity will be time independent. From this we deduced that the kinetic energy of the zonal flow consists of two parts, one which is time dependent and one which is not. Only the time dependent part may be converted into eddy kinetic energy. Hence, there is a lower bound to the amount of energy that may be transformed into eddy kinetic energy. We shall now see that if we require $\partial u/\partial t \equiv 0$ at $y = 0$ and $y = D$ this implies that the mean zonal vorticity is time independent, and that, in a way similar to what we did with the kinetic energy, we may use this time independence to establish a lower boundary on the amount of zonal enstrophy that may be converted into eddy enstrophy.

$$\bar{\zeta}_M = \frac{1}{D}\int_o^D \bar{\zeta}\,dy = -\frac{1}{D}\int_o^D \frac{\partial \bar{u}}{\partial y}\,dy ,$$

$$\frac{d\bar{\zeta}_M}{dt} = \frac{1}{D}\int_o^D \frac{\partial}{\partial y}\left(\frac{\partial \bar{u}}{\partial t}\right)dy = \frac{1}{D}\left\{\left(\frac{\partial \bar{u}}{\partial t}\right)_D - \left(\frac{\partial \bar{u}}{\partial t}\right)_o\right\} = \frac{d}{dt}\left\{\frac{\bar{u}_D - \bar{u}_o}{D}\right\} .$$

Hence, if the zonal velocity does not change with time at the boundaries then $d\bar{\zeta}_M/dt = 0$. The zonal enstrophy is

$$V_Z = \frac{1}{2D}\int_o^D \bar{\zeta}^2\,dy . \tag{4.10}$$

Writing $\bar{\zeta} = \bar{\zeta}_M + \bar{\zeta}'$, we see that this integral separates into

$$V_Z = \frac{1}{2}\bar{\zeta}_M^2 + \frac{1}{2D}\int_o^D (\bar{\zeta}')^2 dy = \frac{1}{2D}(\bar{u}_D - \bar{u}_o)^2 + \frac{1}{2D}\int_o^D (\bar{\zeta}')^2 dy . \tag{4.10a}$$

From this expression we conclude that

$$V_{ZAV} = \frac{1}{2D}\int_o^D (\bar{\zeta} - \bar{\zeta}_M)^2 dy . \tag{4.11}$$

Hence, $V_{ZAV} \neq V_Z$ whenever the zonal velocity at the southern and northern boundary is different and these velocities are kept constant in time. If they are constant in time and equal $\bar{\zeta}_M = 0$ and $V_{ZAV} = V_Z$, which means that all of the zonal enstrophy may be converted into eddy enstrophy.

In both of the models which were constructed in the previous chapter the zonal velocities are kept constant along the two rigid boundaries. Moreover, the value of the velocity along the northern boundary is, in each model, the same as it is along the southern boundary. Hence, from the formula (4.11) we

see that for both models $V_{ZAV} = V_Z$. Later we shall show that the condition $d\bar{u}_M/dt$ puts a further restriction on the transfer of both energy and enstrophy in the case of the simple model so that both the amounts of available energy and enstrophy are actually smaller than what we get from the formulas (4.7) and (4.11).

We have already applied formula (4.11) to the two models that we derived in Chapter 3. This we may do because the streamfunction that we have used in the current chapter is quite general except that it has to satisfy certain boundary conditions. The boundary conditions that we have imposed on our models are equivalent to the boundary conditions that we have used in this chapter. Hence, both models are special cases of the general one that we have worked on in this chapter and all formulaes derived here apply to the two models of Chapter 3.

Using (3.2) and (3.3) we get for the simple model

$$K_Z = \frac{1}{2}(B+C)^2 + \frac{1}{4}(B^2+C^2), \tag{4.12}$$

$$K_E = \frac{1}{8}\left(\frac{\lambda^2+k^2}{k^2}\right)(E_1^2+F_1^2) + \frac{1}{8}\left(\frac{(3\lambda)^2+k^2}{k^2}\right)(E_3^2+F_3^2), \tag{4.13}$$

$$\{K_Z,K_E\} = -\frac{\lambda^2}{k}(B-C)(E_1F_3 - E_3F_1), \tag{4.14}$$

$$K_{ZAV} = \frac{1}{4}(B^2+C^2), \tag{4.15}$$

$$V_Z = \lambda^2B^2 + 4\lambda^2C^2, \tag{4.16}$$

$$V_E = \frac{1}{8}\frac{(\lambda^2+k^2)^2}{k^2}(E_1^2+F_1^2) + \frac{1}{8}\frac{((3\lambda)^2+k^2)^2}{k^2}(E_3^2+F_3^2), \tag{4.17}$$

$$\{V_Z,V_E\} = -\frac{\lambda^2}{k}((2\lambda)^2B - (4\lambda)^2C)(E_1F_3 - E_3F_1), \tag{4.18}$$

$$V_{ZAV} = \lambda^2B^2 + 4\lambda^2C^2 = V_Z. \tag{4.19}$$

For the second model we get by using (3.7):

$$K_Z = \frac{1}{2D}\int_0^D u^2 dy\,, \tag{4.20}$$

$$K_E = \frac{1}{4D}\int_0^D \left\{\frac{1}{k^2}\left(\frac{\partial V_C}{\partial y}\right)^2 + \frac{1}{k^2}\left(\frac{\partial V_S}{\partial y}\right)^2 + V_C^2 + V_S^2\right\} dy\,, \tag{4.21}$$

$$\{K_Z, K_E\} = \frac{1}{2Dk}\int_0^D \bar{u}\{V_S W_C - V_C W_S\}dy\,, \tag{4.22}$$

$$K_{ZAV} = \frac{1}{2D}\int_0^D (\bar{u}-\bar{u}_M)^2 dy\,, \tag{4.23}$$

$$V_Z = \frac{1}{2D}\int_0^D \left(\frac{\partial \bar{u}}{\partial y}\right)^2 dy\,, \tag{4.24}$$

$$V_E = \frac{1}{4Dk}\int_0^D (W_S^2 + W_C^2)dy\,, \tag{4.25}$$

$$\{V_Z, V_E\} = -\frac{1}{2kD}\int_0^D \frac{\partial^2 \bar{u}}{\partial y^2}\{V_S W_C - V_C W_S\}dy\,, \tag{4.26}$$

$$V_{ZAV} = \frac{1}{2D}\int_0^D \left(\frac{\partial \bar{u}}{\partial y}\right)^2 dy = V_Z\,. \tag{4.27}$$

In Chapter 2 we saw that the energy and enstrophy may be separated into the amounts of energy and enstrophy on the different wave numbers. Also we found that the total enstrophy is given by the sum of the products of the energy components and their corresponding two-dimensional wave numbers. This separation of energy and enstrophy into wave number components and the relation between total energy and total enstrophy is easily demonstrated for the simple model. As we have said already we have in this model the two wave numbers 0 and 1 in the zonal direction and 0, 1, 2, 3, 4 in the north-south direction. Hence, using subscripts to indicate wave numbers, equation (4.12) may be written

$$K_Z = K_{0,0} + K_{0,2} + K_{0,4}\,, \tag{4.12a}$$

where

$$K_{0,0} = \frac{1}{2}(B+C)^2, \qquad K_{0,2} = \frac{1}{4}B^2, \qquad K_{0,4} = \frac{1}{4}C^2.$$

Likewise, (4.13) may be written:

$$K_E = K_{1,1} + K_{1,3} \qquad \begin{cases} K_{1,1} = \frac{1}{8}\left(\frac{\lambda^2+k^2}{k^2}\right)(E_1^2+F_1^2) \\ K_{1,3} = \frac{1}{8}\left(\frac{9\lambda^2+k^2}{k^2}\right)(E_3^2+F_3^2) \end{cases} \tag{4.13a}$$

In the same way (4.16) and (4.17) become

$$V_Z = (2\lambda)^2 K_{0,2} + (4\lambda)^2 K_{0,4}, \tag{4.16a}$$

$$V_E = (\lambda^2+k^2)K_{1,1} + ((3\lambda)^2+k^2) K_{1,3}. \tag{4.17a}$$

We will now return to the questions about how much of the zonal energy is available for conversion into eddy energy and how much zonal enstrophy is available for the same conversion. By the principle that only the time dependent part of the zonal kinetic energy is available for conversion we have found that for the simple model

$$K_{ZAV} = \frac{1}{4}(B^2+C^2). \tag{4.15}$$

To get at this formula we had to establish that $\bar{u}_M$ is independent of time. In the case of the simple model $\bar{u}_M$ is given by

$$\bar{u}_M = B + C. \tag{4.28}$$

Hence, the changes in time of B and C are not independent. Due to this we may assume that K_{ZAV} may have a minimum value which is different from zero. In that case K_{ZAV} in the way it is now defined is not the proper zonal available energy. The actual amount will be the difference between K_{ZAV} as it is now defined and the minimum value of this quantity. The minimum value is obtained by using the calculus of variation:

$$\delta K_{ZAV} = \frac{1}{2}(B\delta B + C\delta C),$$

$$\delta C = -\delta B,$$

$$\delta K_{ZAV} = \frac{1}{2}(B-C)\delta C.$$

Hence, $\delta K_{ZAV} = 0$ when $B = C = \bar{u}_M/2$. The minimum value of K_{ZAV} when $B = C$ is $\bar{u}_M/8$. This gives for the amount of zonal energy that is really available for conversion into eddy energy

$$K_{ZAV} = \frac{1}{4}(B^2 + C^2) - \frac{\bar{u}_M^2}{8}.$$

Using (4.28) this may be written

$$K_{ZAV} = \frac{1}{8}(B-C)^2. \tag{4.29}$$

Note that (4.29) is a redefinition of K_{ZAV} and does not correspond to (4.15). In a similar way we shall also show that (4.28) imposes a minimum value which is different from zero on V_{ZAV} as it is defined by (4.19).

$$\delta V_{ZAV} = \lambda^2 2B\delta B + 8\lambda^2 C\delta C,$$

$$\delta C = -\delta B,$$

$$\delta V_{ZAV} = 2\lambda^2(B - 4C)\delta C.$$

Hence, $\delta V_{ZAV} = 0$ when $B = 4C = (4/5)\bar{u}_M$. Again using (4.28) we find that V_{ZAV} should be redefined to be

$$V_{ZAV} = \frac{\lambda^2}{5}(B - 4C)^2. \tag{4.30}$$

From that we have just done we see that the fact that the total zonal momentum in the simple model is expressed only in terms of B and C puts an extra constraint on the transfer of energy in this model in addition to the constraint we get from the conservation of total zonal momentum. With more degrees of freedom for the zonal flow this additional constraint will not come into play.

From formulaes (4.4) and (4.9) we see that the quantity $(\partial/\partial y)\overline{(u'v')}$ is essential for both the exchange of energy and enstrophy between the eddies and the zonal flow. This quantity expresses the divergence of the zonally averaged momentum transport. By using the streamfunction for the simple model we find that the divergence of momentum transport in this model may be written

$$\frac{\partial}{\partial y}\overline{(u'v')} = \frac{2\lambda^2}{k}(E_1F_3 - E_3F_1)(\cos(2\lambda y) - \cos(4\lambda y)).$$

For later use the term $E_1F_3 - E_3F_1$ will be denoted by M. From the expression we have just obtained we see that the sign of M determines where we will have convergence or divergence. Formula (4.14) may now be written:

$$\{K_Z, K_E\} = -\frac{\lambda^2}{k}(B-C)M. \qquad (4.14a)$$

This formula tells us that the direction of the energy flow in the simple model is determined by the signs of the two terms B-C and M. We see that when $B > C$ we must have $M < 0$ to get a conversion of zonal energy into eddy energy. If $B < C$ we must have $M > 0$ in order to get the same conversion. The reason for this may be explained as follows: When $B > C$ the zonal velocity field will have a more or less pronounced single jet structure. How pronounced this structure is depends on how much greater B is than C. On Figure 4.1 we have showed a graph of the function

$$F(y) = \cos(2\lambda y) - \cos(4\lambda y).$$

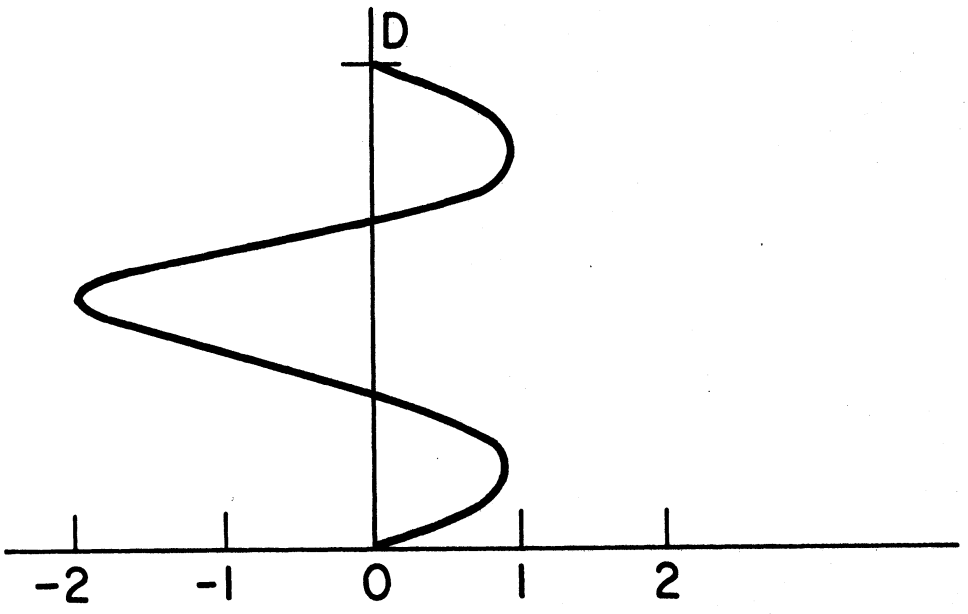

Figure 4.1. Graph of the function $\cos(2\lambda y) - \cos(4\lambda y)$.

When $M < 0$ we see from the graph that there will be a divergence of momentum transport at the center of the channel and a convergence to the north and the

south of the center, thus indicating that momentum is being transported away from the zone where the zonal wind is strongest. The zonal wind here decreases and it increases to the north and to the south. The zonal wind field is thus changing its shape and the value of the zonal wind is everywhere getting closer to its mean value. This implies that the zonal kinetic energy is decreasing, because it is the deviation of the zonal wind field from its mean value that determines the amount by which the zonal kinetic energy exceeds its mean value.

When $C > B$ the zonal wind field will have a more or less pronounced double jet structure. There will be one jet to the north of the center of the channel and one to the south. From what we have already said it is easily recognized that the sign of M must now be opposite to what it was in the previous case if we want the same conversion of energy to occur, because now we want a transport of momentum towards the center. As in the previous case this transport of momentum will reduce the deviations of the zonal wind from its mean value, which implies that the zonal kinetic energy will decrease, which in its turn implies an increase of eddy kinetic energy.

Some information on how this transport of momentum comes about may be obtained if we calculate the slope of the trough and ridge lines. In the simple model the streamfunction describing the eddy flow is

$$\psi'(x,y,t) = \frac{1}{k}\{E_1(t)\sin \lambda y + E_3(t)\sin 3\lambda y\}\sin kx + \frac{1}{k}\{F_1(t)\sin \lambda y + F_3(t)\sin 3\lambda y\}\cos kx .$$

Let us for simplicity write this streamfunction as

$$\psi'(x,y,t) = L_1(y,t)\sin(kx) + L_2(y,t)\cos(kx) .$$

At the trough and the ridge we must have

$$v = \frac{\partial \psi'}{\partial x} = k\{L_1 \cos(kx) - L_2 \sin(kx)\} = 0 .$$

Hence, we have the equation

$$\frac{L_1}{L_2} - \tan(kx) = 0 \qquad (4.31)$$

By differentiating this we get

$$\frac{\frac{dL_1}{dy}L_2 - \frac{dL_2}{dy}L_1}{L_2^2}\,dy - \frac{k}{\cos^2(kx)}\,dx = 0,$$

or

$$\frac{dy}{dx} = \frac{kL_2^2}{\cos^2(kx)} \cdot \frac{1}{\frac{dL_1}{dy}L_2 - \frac{dL_2}{dy}L_1}$$

After we have substituted for $\cos^2 kx$ from (4.31), expressing $\cos^2 kx$ in terms of $tg^2 kx$, and also calculated the term $(dL_1/dy)L_2 - (dL_2/dy)L_1$ from the definition of L_1 and L_2, we find that dy/dx may be written:

$$\frac{dy}{dx} = \frac{k^3(L_1^2 + L_2^2)}{2\lambda(1 - \cos(2\lambda y))} \cdot \frac{1}{M \sin(2\lambda y)} \qquad (4.32)$$

From this expression we see that the sign of dy/dx depends only on M and $\sin(2\lambda y)$ $(\sin((2\pi/D)y))$. The first case we discussed above had $M < 0$. In this case the streamline pattern will look as it does on Figure 4.2. With

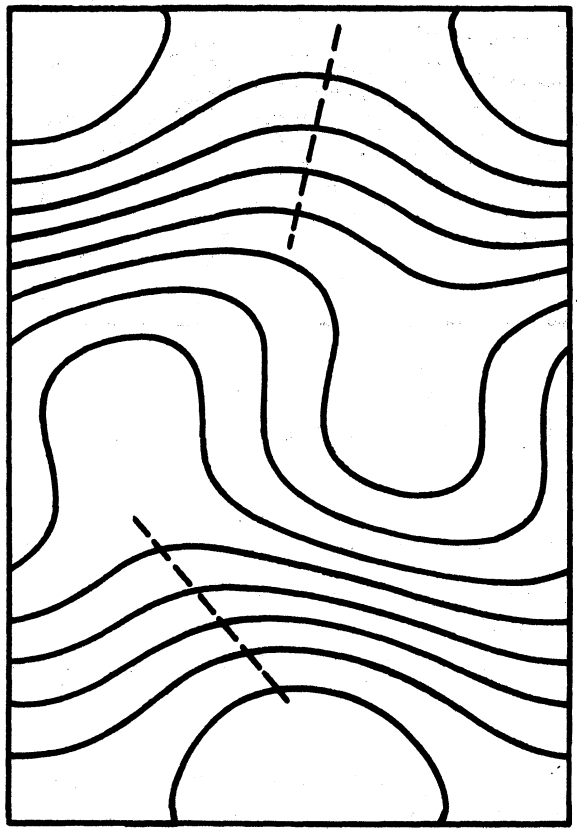

Figure 4.2. Streamfield when $M < 0$. The eddy flow is superposed on a zonal flow defined by $\bar{u}(y) = 15(1 - \cos(4\lambda y))$.

this tilt of the ridge and trough lines the eddy flow will transport momentum away from the center of the channel. There is a northward transport of momentum north from the center of the channel because northward-moving air particles are associated with a greater west-wind component than are southward-moving particles. At the southern side the transport is caused by the southward-moving particles having a greater westward-wind component than northward-moving particles. In the case when $M > 0$ which was the case when we needed a momentum transport toward the center of the channel in order for the eddy kinetic energy to grow, the streamlines will be similar to what they are on Figure 4.3. Here

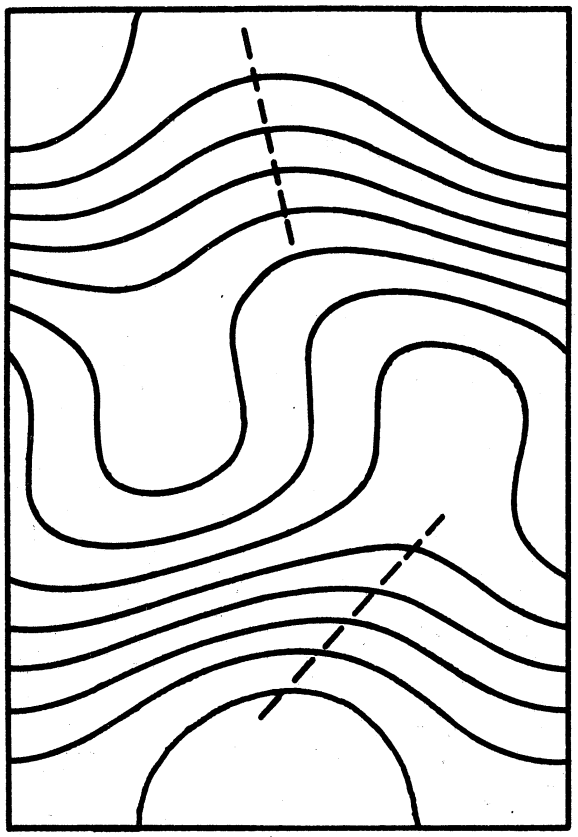

Figure 4.3. Streamfield when $M > 0$. The eddy flow is superposed on a zonal flow defined by $\bar{u}(y) = 15(1 - \cos(4\lambda y))$.

one finds that the southward-moving particles have the greatest westward-wind component in the northern half of the channel, and the northward-moving particles have the greatest westward-wind component in the southern half of the channel, thus giving rise to a net transport of momentum towards the center of the channel.

To sum up, we have found that the conversion of zonal kinetic energy into eddy kinetic energy is accomplished by the transport of momentum by the eddies. For this transport to occur it is essential that the trough and ridge lines are tilted, i.e., their orientation is not strictly along the parallels.

In the above discussion we have concentrated on the conversion from zonal to eddy kinetic energy. Of course, the same kind of mechanism that we have just outlined is responsible also for the opposite conversion to occur.

CHAPTER 5

DERIVING AN ALTERNATIVE SET OF EQUATIONS FOR THE SIMPLE MODEL

In Chapter 4 we defined the quantities $K_{1,1}$, $K_{1,3}$, and M; where $K_{1,1}$ and $K_{1,3}$ are the energies on the wave numbers 1,1 and 1,3 of the eddy flow, respectively, and M is proportional to the divergence of momentum transport. From the system of equations (3.5) we may now derive an equivalent set of equations where $K_{1,1}$, $K_{1,3}$, and M are among the dependent variables. This new set of equations is:

$$\frac{dB}{dt} = 2kQM\,,$$

$$\frac{dC}{dt} = -2kQM\,,$$

$$\frac{dK_1}{dt} = -k\left[\frac{5Q+1}{2(1+Q)}\,B + \frac{7Q-1}{2(1+Q)}\,C\right]M\,,$$

$$\frac{dK_3}{dt} = -k\left[\frac{3Q-1}{2(1+9Q)}\,B - \frac{15Q-1}{2(1+9Q)}\,C\right]M\,,$$

$$\frac{dM}{dt} = -k\left\{\left[\frac{3Q-1}{1+9Q}\,B - \frac{15Q-1}{1+9Q}\,C\right]K_1 + \left[\frac{5Q+1}{1+Q}\,B + \frac{7Q-1}{1+Q}\,C\right]K_3 + \left[\frac{3Q-1}{2(1+Q)}\,B + \frac{8Q}{(1+9Q)(1+Q)}\,R\right]N\right\}\,,$$

$$\frac{dN}{dt} = k\left[\frac{3Q-1}{2(1+Q)}\,B + \frac{8Q}{(1+9Q)(1+Q)}\,R\right]M\quad. \tag{5.1}$$

Here $Q = \lambda^2/k^2$, $R = \beta/k^2$, and $N = E_1E_3 + F_1F_3$. For simplicity we have written K_1 and K_3 instead of $K_{1,1}$ and $K_{1,3}$. Also in later chapters we shall stick to this notation, except in cases when it may give rise to confusion. Comparing (3.5) and (5.1) we see that the latter is simpler. It also gives us directly the quantities we are interested in. For these reasons we will rather use (5.1) than (3.5). We notice that the first two equations are the same in (5.1) as they are in (3.5). In the previous chapter we found that $B + C = \bar{u}_M$, and also that $d\bar{u}_M/dt = 0$. Hence, one of these equations may be replaced by a diagnostic equation which simply gives B (or C) as the difference between $\bar{u}_M$ and C (or B). One can also show that the dependent variable N may be calculated from a diagnostic equation, and that it is in fact, not independent of the other eddy variables. This we may do in the following way: The four equation for the eddy quantities may be written:

$$\frac{dK_1}{dt} = -\frac{1}{2} k\alpha M ,$$

$$\frac{dK_3}{dt} = -\frac{1}{2} k\beta M ,$$

$$\frac{dM}{dt} = -k\{\beta K_1 + \alpha K_3 + \gamma N\} ,$$

$$\frac{dN}{dt} = k\gamma M , \qquad (5.2)$$

where

$$\alpha = \frac{5Q+1}{1+Q} B + \frac{7Q-1}{1+Q} C ,$$

$$\beta = \frac{3Q-1}{1+9Q} B - \frac{15Q-1}{1+9Q} C ,$$

$$\gamma = \frac{3Q-1}{2(1+Q)} B + \frac{8Q}{(1+9Q)(1+Q)} R . \qquad (5.3)$$

In general, $\alpha = \alpha(t)$, $\beta = \beta(t)$, and $\gamma = \gamma(t)$ because $B = B(t)$ and $C = C(t)$. Under these general conditions one may write:

$$\alpha = -\frac{2}{kM}\frac{dK_1}{dt} ,$$

$$\beta = -\frac{2}{kM}\frac{dK_3}{dt} ,$$

$$\gamma = \frac{1}{kM}\frac{dN}{dt} . \qquad (5.4)$$

Substituting from these expressions for α, β, and γ into the third equation of (5.2) we get

$$\frac{dM}{dt} = -k\left\{-K_1 \frac{2}{kM}\frac{dK_3}{dt} - K_3 \frac{2}{kM}\frac{dK_1}{dt} + N \frac{1}{kM}\frac{dN}{dt}\right\}$$

which also may be written:

$$M\frac{dM}{dt} = 2K_1 \frac{dK_3}{dt} + 2K_3 \frac{dK_1}{dt} - N\frac{dN}{dt} ,$$

or

$$N^2 = 4K_1K_3 - M^2. \tag{5.5}$$

N should therefore be considered as a convenient dependent variable, but it does not have a separate dynamical meaning or interpretation. As a matter of fact (5.5) could be used to disregard one of the four equations for the eddy variables although we did not do that in our minimum integrations.

It is naturally also possible to show (5.5) by direct algebraic manipulations, i.e., to prove the identity

$$4 \cdot \frac{1}{2}(E_1^2+F_1^2) \cdot \frac{1}{2}(E_3^2 + F_3^2) - (E_1F_3 - E_3F_1)^2 = (E_1E_3 + F_1F_3)^2,$$

as is easily done.

CHAPTER 6

LINEAR STABILITY ANALYSIS

In this chapter we will carry out a linear stability analysis of both models. Also we shall demonstrate that stability in the linear sense seems to be related to the nonlinear properties of the models. In the case of the extended one the stability analysis will only be an approximative one. This because we are not going to allow the flow to have a completely general variation in the y-direction, but rather restrict its variation to be made up from only a few Fourier-components. For the zonal flow we assume a profile of the form (3.1); which is, as one can see, the same zonal wind profile as we have for the simple model. The eddy flow we allow to have three wave numbers in the y-direction: λ, 3λ, and 5λ. Thus the only difference between this model and the simple one is the wave number 5λ of the eddy flow. For the sake of brevity the linear stability analysis of the model including the wave number 5λ will be called the analysis of the extended model, understanding that it is an approximation.

For the linear stability analysis of the simple model we take as our starting point the equations (5.1). The linearization is done by leaving out the first two equations and by regarding B and C as independent of time in the rest of the equations. Using the notation we have defined in (5.3) we get

$$\begin{aligned}
\frac{dK_1}{dt} &= -\frac{k\alpha}{2} M, \\
\frac{dK_3}{dt} &= -\frac{k\beta}{2} M, \\
\frac{dM}{dt} &= -k(\beta K_1 + \alpha K_3 + \gamma N), \\
\frac{dN}{dt} &= k\gamma M. \qquad (6.1)
\end{aligned}$$

These equations are all linear because α, β, and γ are all independent of time. The equations (6.1) may be combined into a single one by taking the second derivative of M with respect to time and then substitute for dK_1/dt, dK_3/dt, and dN/dt from the other equations. The single equation that we then get, is

$$\frac{d^2M}{dt^2} + k^2(\gamma^2 - \alpha\beta)M = 0$$

This equation, we know, will have trigonometric solutions if

$$\gamma^2 > \alpha\beta , \tag{6.2}$$

in which case the flow is said to be stable. If, on the other hand,

$$\gamma^2 < \alpha\beta , \tag{6.3}$$

we will get exponential solutions; and the flow is said to be unstable. From (6.2) we see that a sufficient condition for stability is that

$$\alpha\beta < 0 . \tag{6.4}$$

This is the condition that will enable us to relate stability in a linear sense to the nonlinear properties of the flow. Note that (6.4) would be the exact condition if we neglected the variation of the Coriolis-parameter in the model.

In the case that the flow is stable we define the period of its motion to be

$$T = \frac{2\pi}{k\sqrt{\gamma^2 - \alpha\beta}} .$$

When it is unstable, the e-folding time of the perturbations is given by:

$$T_* = \frac{1}{k\sqrt{\alpha\beta - \gamma^2}} .$$

Results from this stability analysis are presented in Table 6.1 and on Figures 6.1-6.3. In the figures we show the combinations of L_x and L_y ($L_y = 2D$) which give instability for given values of B and C. Isolines are drawn through points having the same e-folding time.

Comparing the Figures 6.1, 6.2, and 6.3 we see that the region of instability changes from one case to the other. Regarding α, β, and γ as functions of L_x and L_y makes it possible to relate the positions of the stability zones to the magnitude of the two-dimensional wave numbers of the simple model. If we use the criterion $\alpha\beta < 0$ for the case shown on Figure 6.1 with B = 30 m/s and C = 0 m/s, this criterion indicate stability whenever $Q < 1/3$; and as one can see from Figure 6.1 the region of instability is situated well below this

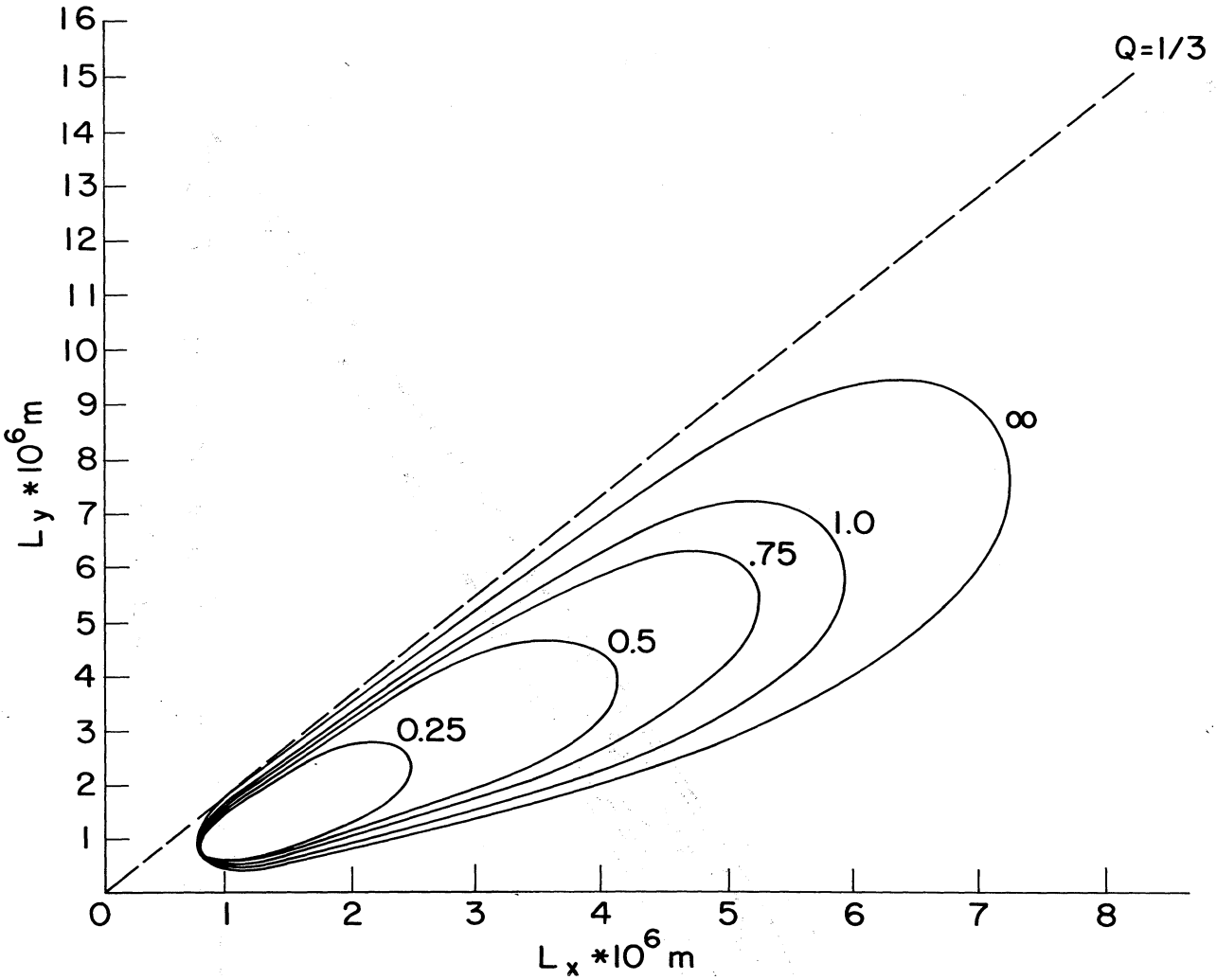

Figure 6.1. Instability diagram for the simple model. Zonal flow defined by B = 30 m/s and C = 0 m/s. Curves are isolines of e-folding time. This is measured in fractions of days.

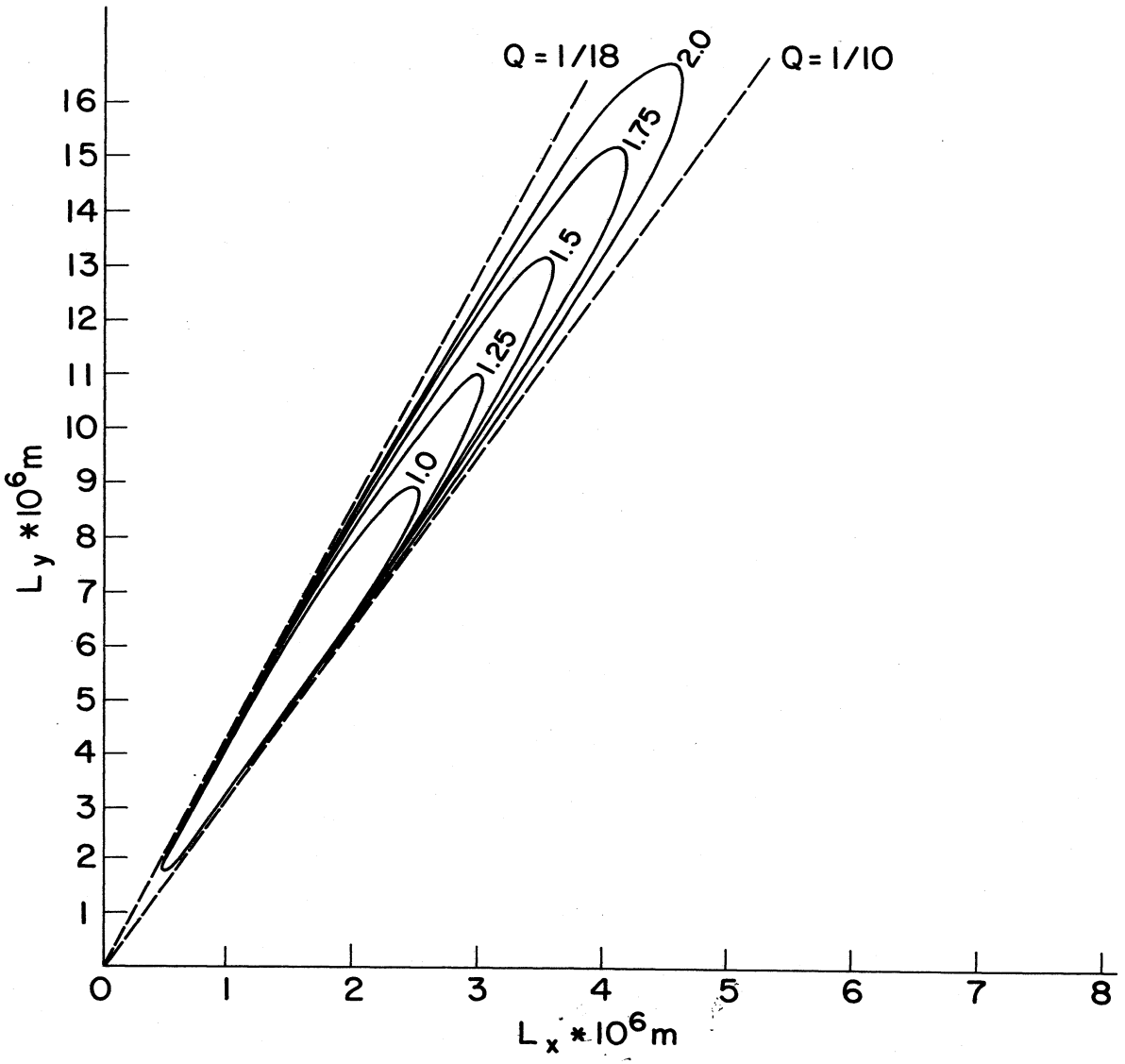

Figure 6.2. Instability diagram for the simple model. Zonal flow defined by B = 5 m/s and C = 25 m/s.

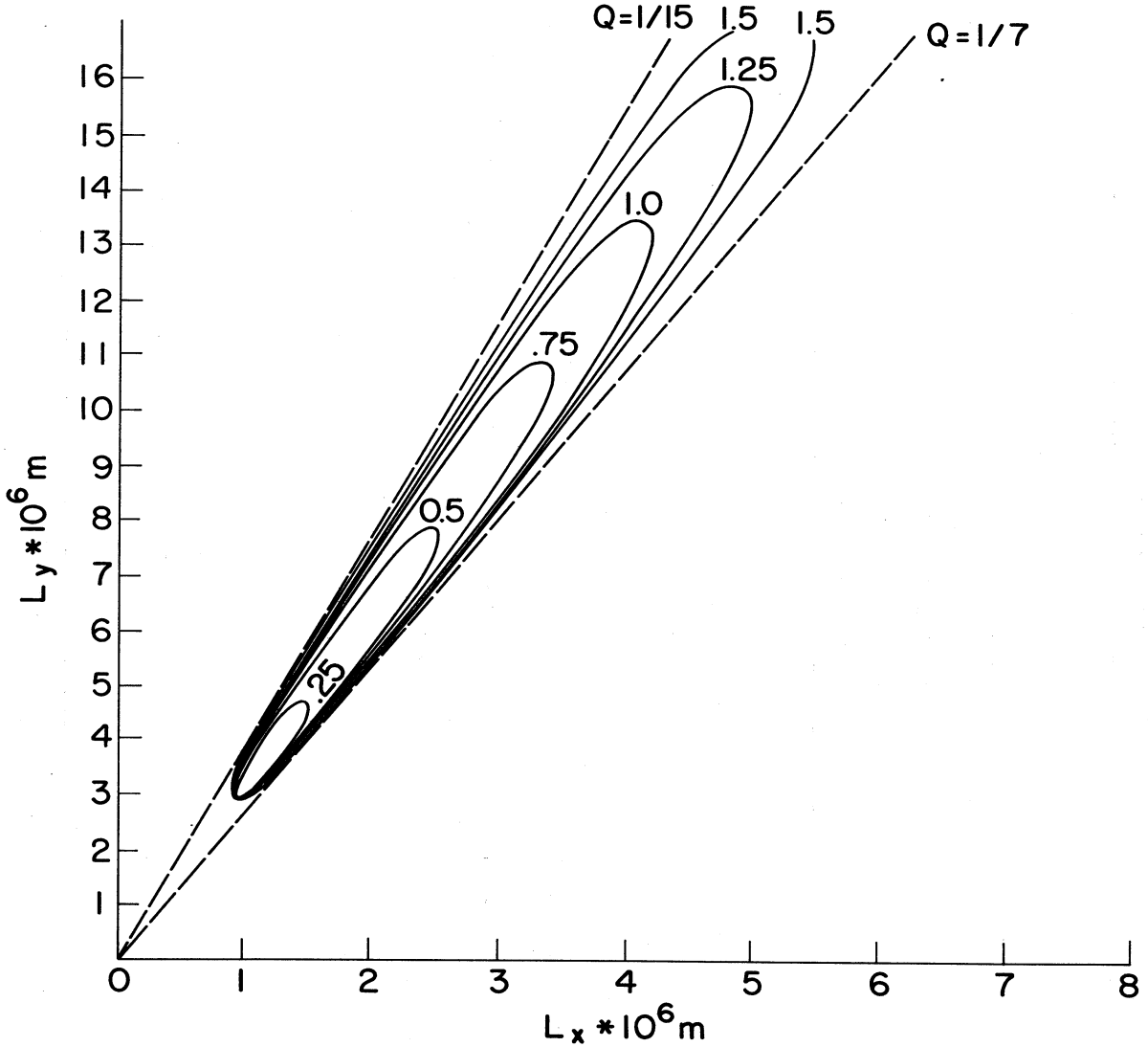

Figure 6.3. Instability diagram for the simple model. Zonal flow defined by B = 0 m/s and C = 30 m/s.

TABLE 6.1

SHOWING FOR WHICH COMBINATIONS OF B AND C INSTABILITIES OCCURRED IN THE SIMPLE AND IN THE EXTENDED MODEL

B(m/s)	C(m/s)	Simple Model	Extended Model
30	0	instabilities	instabilities
25	5	no instabilities	instabilities
20	10	no instabilities	instabilities
15	15	no instabilities	instabilities
10	20	no instabilities	instabilities
5	25	instabilities	instabilities
0	30	instabilities	instabilities

line, corresponding to values of Q being greater than 1/3. We may now compare the value Q = 1/3 to some of the values listed in Table 6.2. Here we have listed the magnitudes of the two-dimensional wave numbers (in units of λ) for different values of Q (the two-dimensional wave number 0 not included). Comparing the three first lines of this table we find that Q = 1/3 is the value that makes $\sqrt{k^2+\lambda^2} = 2\lambda$, Q > 1/3 makes $\sqrt{k^2+\lambda^2} < 2\lambda$, and Q < 1/3 makes $\sqrt{k^2+\lambda^2} > 2\lambda$. Since $\sqrt{k^2+9\lambda^2}$ will always be greater than both $\sqrt{k^2+\lambda^2}$ and 2λ, these results suggest that we will get stability when the wave number of the zonal flow is smaller than the two-dimensional wave numbers of the eddies that interact with it, and that, on the other hand, instability might be favored when the zonal wave number lies between the eddy-wave numbers.

TABLE 6.2

MAGNITUDE OF THE EDDY WAVE NUMBERS RELATED TO THE ZONAL WAVE NUMBERS FOR DIFFERENT VALUES OF Q

Q	2λ	4λ	$\sqrt{k^2+\lambda^2}$	$\sqrt{k^2+9\lambda^2}$	L_y/L_x
1/2	2λ	4λ	$\sqrt{3}\lambda$	$\sqrt{11}\lambda$	$\sqrt{2}$
1/3	$\underline{2\lambda}$	4λ	$\underline{2\lambda}$	$2\sqrt{3}\lambda$	$\sqrt{3}$
1/4	2λ	4λ	$\sqrt{5}\lambda$	$\sqrt{13}\lambda$	2
1/7	2λ	$\underline{4\lambda}$	$2\sqrt{2}\lambda$	$\underline{4\lambda}$	$\sqrt{7}$
1/10	2λ	4λ	$\sqrt{11}\lambda$	$\sqrt{19}\lambda$	$\sqrt{10}$
1/15	2λ	$\underline{4\lambda}$	$\underline{4\lambda}$	$2\sqrt{6}\lambda$	$\sqrt{15}$
1/20	2λ	4λ	$\sqrt{21}\lambda$	$\sqrt{29}\lambda$	$\sqrt{19}$

Remembering that C = 0 in this case, so that there is no initial energy on wave number 4λ of the zonal flow, it is clear why the relation between the eddy wave numbers and wave number 2λ of the zonal flow is important in this case.

In the next case, which has B = 5 m/s, C = 25 m/s, we find that there is always stability when $Q > 1/10$ when $Q < 1/18$. These values are not as easily related to the magnitude of the wave numbers. The reason for this being of course that because we now initially have energy on both the zonal wave numbers, there will be a cascade both up and down the wave number spectrum, even if the eddy wave numbers are not symetrically placed around any of the two zonal wave numbers.

The last case with the simple model has B = 0 m/s and C = 30 m/s; which means that all the zonal energy initially is in wave number 4λ. Here our assumption that instability is favored when energy may be cascaded away from the zonal wave number towards both a higher and a lower wave number, is confirmed. The criterion $\alpha\beta < 0$ gives us the values $Q = 1/7$ and $Q = 1/15$ for the stability boundaries, and from Table 6.2 we find that $1/15 < Q < 1/7$ corresponds to a range in which the eddy wave numbers have values which make one of them larger and the other one smaller than 4λ.

The approximate analysis of the extended model is carried out in the following way: The linearized version of the barotropic vorticity equation is

$$\nabla^2 \frac{\partial \psi'}{\partial t} + \bar{u} \frac{\partial}{\partial x} (\nabla^2 \psi') + \left(\beta - \frac{d^2 \bar{u}}{dy^2} \right) \frac{\partial \psi'}{\partial x} = 0 \qquad (6.5)$$

Here $\psi' = \psi'(x,y,t)$ is the streamfunction of the perturbations, and $\bar{u} = \bar{u}(y)$ is the zonal flow; which is kept constant with time but allowed to vary with y. In both models that we consider the variation in the x-direction is expressed by one single Fourier-component. Using this we may write the perturbation streamfunction in the following way:

$$\psi'(x,y,t) = \alpha(y)\, e^{i\mu(x-ct)} \qquad (6.6)$$

Substituting this into (6.5) we get:

$$(\bar{u}-c) \left[\frac{d^2\alpha}{dy^2} - \mu^2 \alpha \right] + \left(\beta - \frac{d^2 \bar{u}}{dy^2} \right) \alpha = 0 \qquad (6.7)$$

Now the problem is reduced to a problem of finding for which profiles of $\bar{u}$ and α we get complex values of c, and for which we get real values. In the numerical integrations that we shall carry out later, we shall always start with the same initial fields for both models. Hence, also for the extended model we are going to assume that the zonal wind intially is given by:

$$\bar{u}(y) = B + C - B\cos(2\lambda y) - C\cos(4\lambda y) \tag{6.8}$$

In the case when we integrate the linearized version of the models this profile is, of course, not going to change during the integration. As mentioned earlier we will restrict α so that it is defined by:

$$\alpha = \sum_n \alpha_n \sin(n\lambda y), \qquad n = 1,3,5 \tag{6.9}$$

By substituting (6.8) and (6.9) into (6.7) we get after a considerable amount of manipulations:

$$\begin{aligned}
(u_1 c + R_1)\alpha_1 + R_2\alpha_3 + R_3\alpha_5 &= 0 \\
R_4\alpha_1 + (u_2 c + R_5)\alpha_3 + R_6\alpha_5 &= 0 \\
R_7\alpha_1 + R_8\alpha_3 + (u_3 c + R_9)\alpha_5 &= 0
\end{aligned} \tag{6.10}$$

Here the u's and the R's are defined by:

$$\begin{aligned}
u_1 &= \mu^2 + \lambda^2 \\
u_2 &= \mu^2 + 9\lambda^2 \\
u_3 &= \mu^2 + 25\lambda^2 \\
R_1 &= \beta - (\mu^2 + \lambda^2)(B+C) - \frac{B}{2}(\mu^2 - 3\lambda^2) \\
R_2 &= \frac{B}{2}(\mu^2 + 5\lambda^2) - \frac{C}{2}(\mu^2 - 7\lambda^2) \\
R_3 &= \frac{C}{2}(\mu^2 + 9\lambda^2) \\
R_4 &= \frac{B}{2}(\mu^2 - 3\lambda^2) - \frac{C}{2}(\mu^2 - 15\lambda^2) \\
R_5 &= \beta - (\mu^2 + 9\lambda^2)(B+C) \\
R_6 &= \frac{B}{2}(\mu^2 + 21\lambda^2)
\end{aligned}$$

$$R_7 = \frac{C}{2}(\mu^2 - 15\lambda^2)$$

$$R_8 = \frac{B}{2}(\mu^2 + 5\lambda^2)$$

$$R_9 = \beta - (\mu^2 + 25\lambda^2)(B+C)$$

For this system to have a nontrivial solution its determinant must equal zero. Calculating the determinant and equating it to zero gives a third order equation in c:

$$c^3 + \left(\frac{R_1}{u_1} + \frac{R_5}{u_2} + \frac{R_9}{u_3}\right)c^2 + \left(\frac{R_1R_5 - R_2R_4}{u_1u_2} + \frac{R_1R_9 - R_3R_7}{u_1u_3} + \frac{R_5R_9 - R_6R_8}{u_2u_3}\right)c +$$

$$+ \frac{1}{u_1u_2u_3}(R_1(R_5R_9 - R_6R_8) + R_2(R_6R_7 - R_4R_9) + R_3(R_4R_8 - R_5R_7)) = 0$$

This equation has been solved numerically for different values of μ, λ, B, and c. For each pair of values of B and C we allowed μ and λ to vary through their whole range of values, thus obtaining diagrams similar to those that we got for the simple model. The results from four cases are shown on Figures 6.4-6.7. Also in Table 6.1 we have summarized all the cases that we worked out. First we note from Table 6.1 that this analysis gave instability in all cases, while the analysis of the simple model only gave instability for some pair of values of B and C. Secondly, from the graphs we see that for the same pair of values of B and C the zones of instability are larger with the extended model than with the simple one, indicating instability over a much wider range of L_x-values for a given L_y-value. Thirdly, we see from Figure 6.7 that the zone of instability in the case of the extended model may consist of two almost entirely separated parts.

On Figure 6.4 we have drawn the line Q = 1/3. The unstable region is well below this line, indicating that as far as stability is concerned the two models may very well be subject to the same rules. In the case of the simple model we related the stability to the condition $2\lambda < \sqrt{k^2+\lambda^2}$. Also in the extended model we may get $2\lambda < \sqrt{k^2+\lambda^2}$ or $2\lambda > \sqrt{k^2+\lambda^2}$, depending on which values of L_x and L_y we use, furthermore $2\lambda < \sqrt{k^2+25\lambda^2}$ for any value of k. Hence, the addition of a new wave number does not seem to have any importance here, and it is reasonable therefore that Q = 1/3 is a common stability boundary in both models. The larger region of instability in the extended model and also that this region is further removed from the stability line, than it is in the case of the simple model, indicate that the conditions for instability are slightly different with the two models. However, still it is true that when we have instability the zonal flow is cascading in both directions. Hence, it seems that our main conclusions are still valid, and that the extra wave number only has changed the results quantitatively.

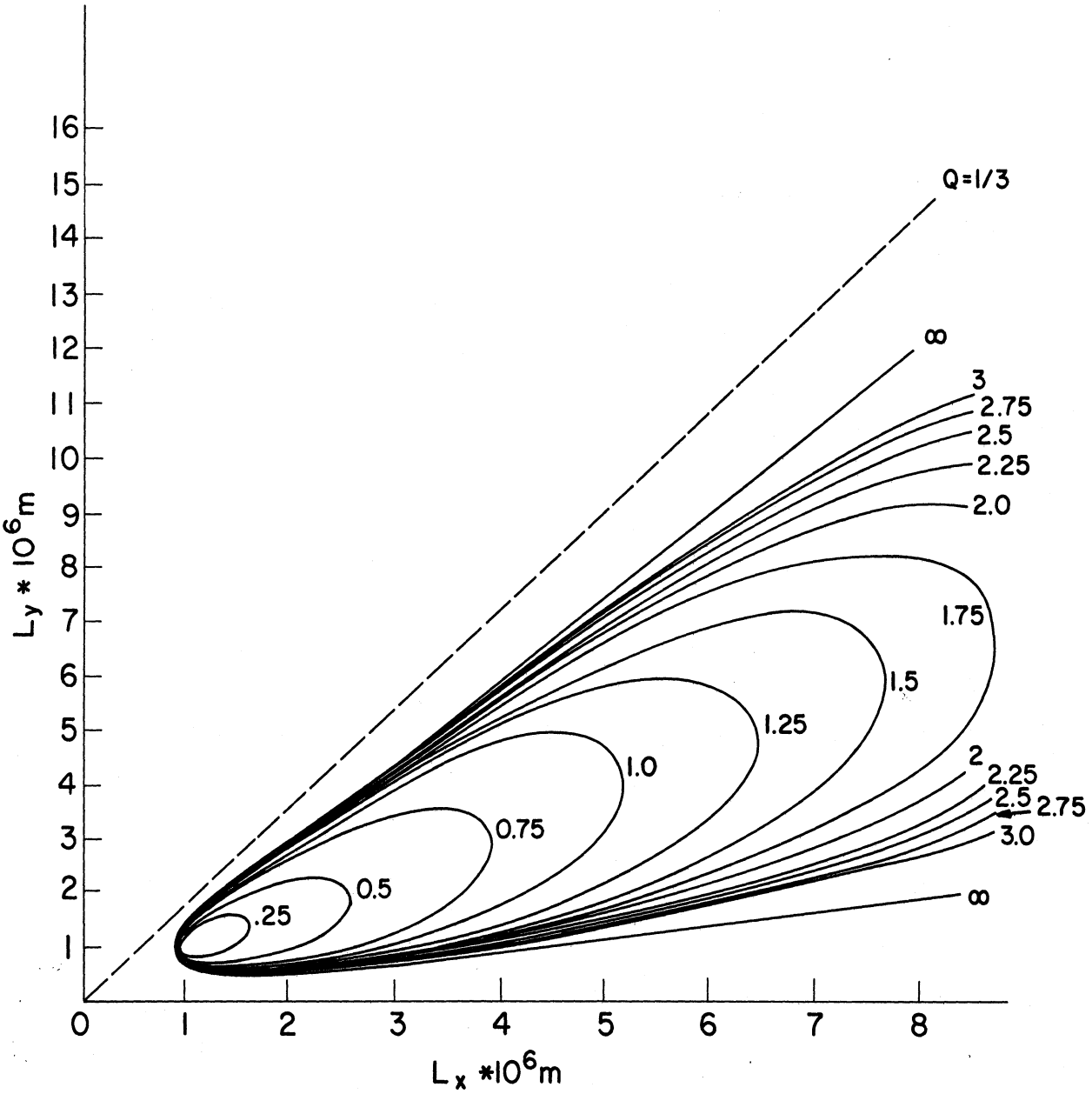

Figure 6.4. Approximate instability diagram for the extended model. Zonal flow defined by B = 0 m/s and C = 30 m/s.

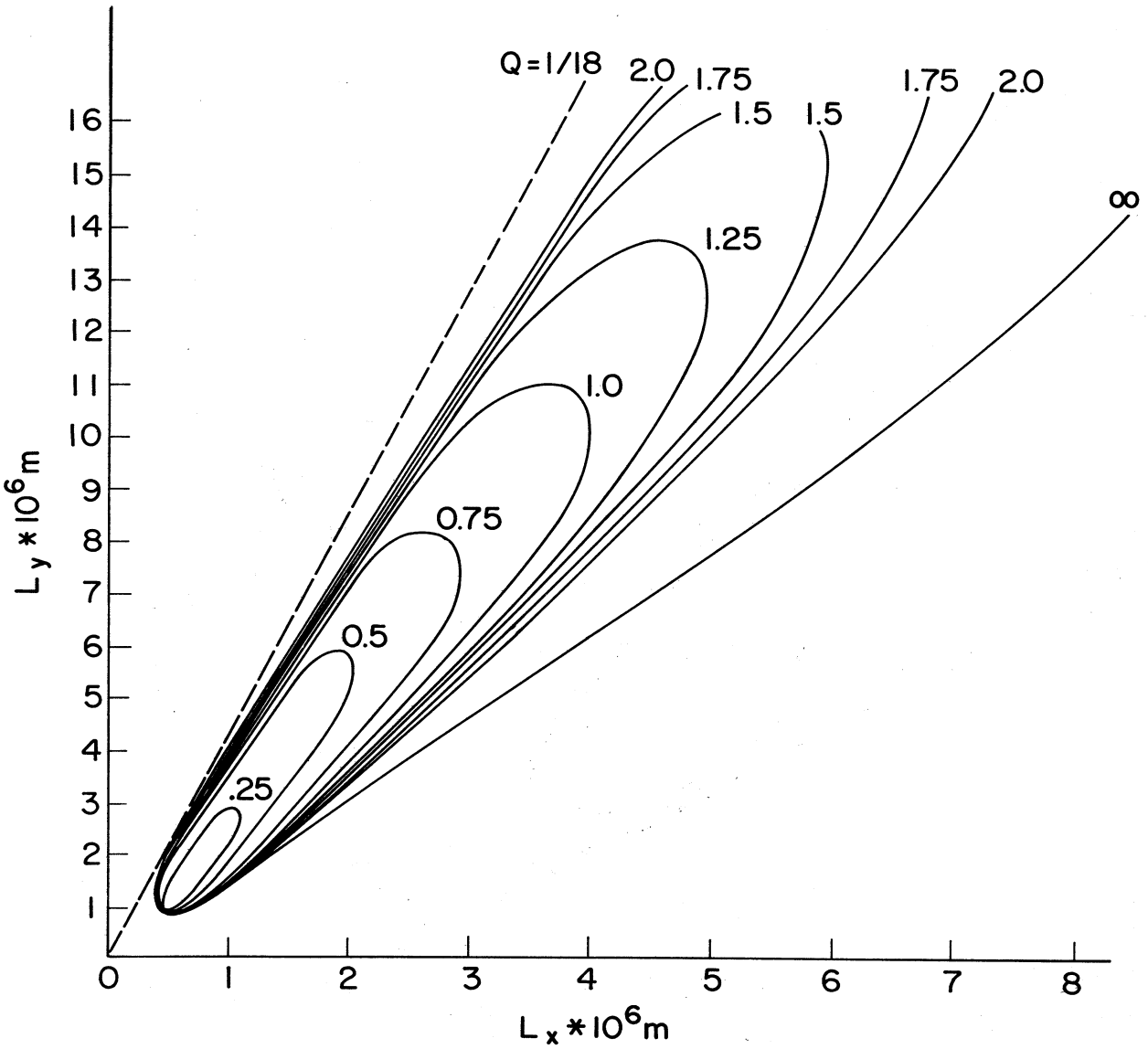

Figure 6.5. Approximate instability diagram for the extended model. Zonal flow defined by B = 5 m/s and C = 25 m/s.

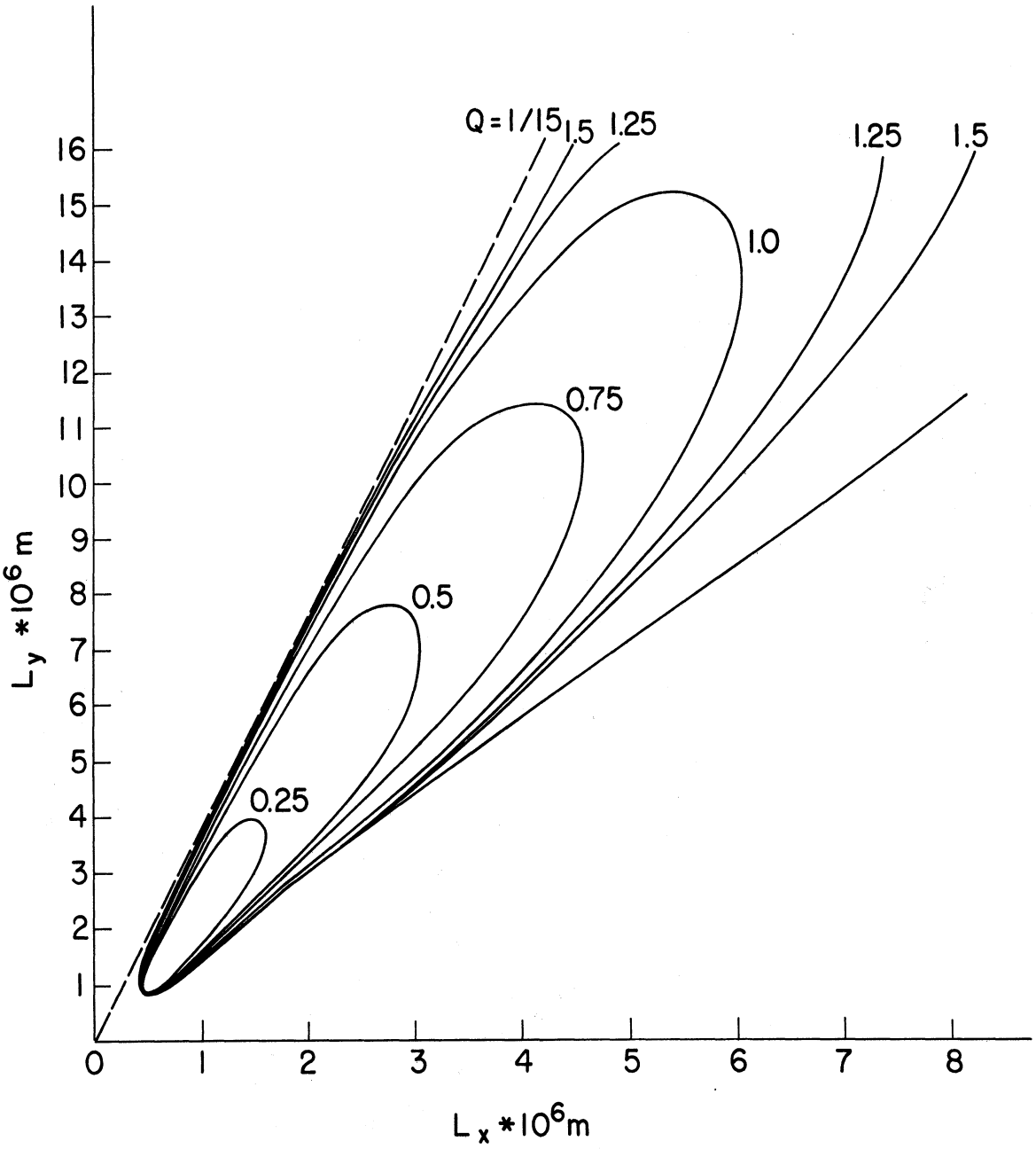

Figure 6.6. Approximate instability diagram for the extended model. Zonal flow defined by B = 0 m/s and C = 30 m/s.

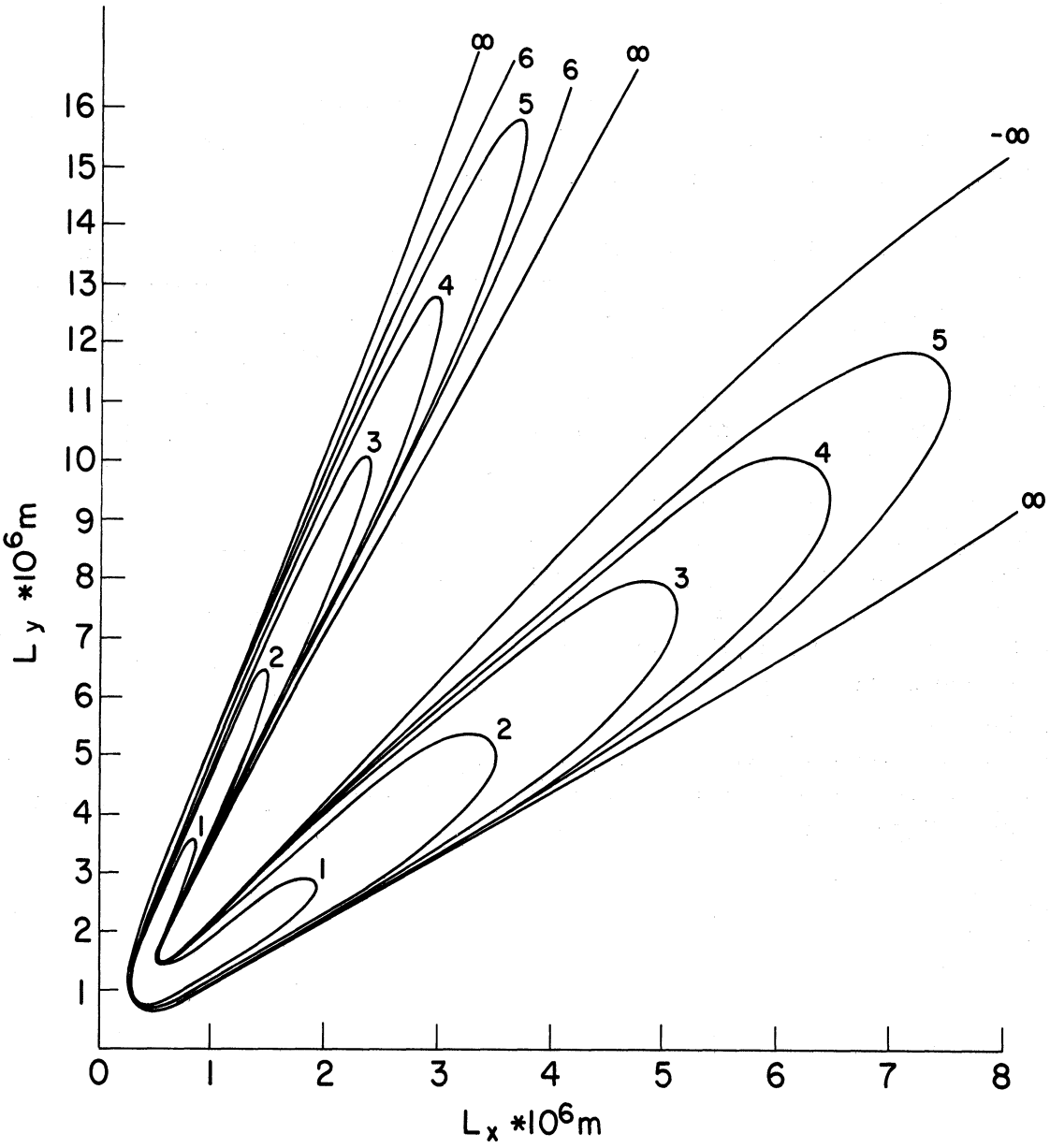

Figure 6.7. Approximate instability diagram for the extended model. Zonal flow defined by B = 15 m/s and C = 15 m/s.

In the next case, having B = 5 m/s and C = 25 m/s, we find that the stability boundary defined by Q = 1/18 which we obtained for the simple model also fits the extended model. The other boundary, given by Q = 1/10, is obviously irrelevant in the case of the extended model.

The last case that we want to discuss has B = 0 m/s and C = 30 m/s. As in the previous case one of the stability boundaries fits both models. This boundary is defined by Q = 1/15. The value Q = 1/15 corresponds to the value when $\sqrt{k^2+\lambda^2} = 4\lambda$. For smaller values of Q we see from Table 6.2 that the magnitude of all the eddy wave numbers are greater than 4λ. For any value of k, $\sqrt{k^2+25\lambda^2} > 4\lambda$. As in the case when B = 30 m/s and C = 0 m/s we have a value of Q that, if it is surpassed, will ensure that all the eddy wave numbers are greater than the zonal wave number. Hence, from the reasoning that stability or instability depends on the magnitude of the wave numbers, the coincidence of the stability boundary in the two models seems reasonable. From Table 6.2 we see that Q > 1/7 is the range of values for which both eddy wave numbers of the simple model are smaller than 4λ. Hence, one would expect stability for Q > 1/7 in the case of the simple model. In the case of the extended model it is impossible for all the eddy wave numbers to be smaller than 4λ. Hence, from the point of view that we will get stability when the eddy wave numbers are either all smaller or all larger than the zonal wave number in question, one should not expect Q = 1/7 to apply for the extended model.

CHAPTER 7

DISCUSSION OF SOME NUMERICAL INTEGRATIONS

For all the integrations to be discussed in this chapter we used the following initial conditions:

$$B = 0 \text{ m/s}$$

$$C = 30 \text{ m/s}$$

$$K_1 = 100 \text{ m}^2/\text{s}^2$$

$$K_3 = 25 \text{ m}^2/\text{s}^2$$

$$M = 0 \text{ m}^2/\text{s}^2$$

$$N = 100 \text{ m}^2/\text{s}^2$$

These values of B and C give us an initial zonal flow that has a double jet structure. At both maxima the velocity is 2C (i.e., 60 m/s). These maxima are situated at $y = D/4$ and at $y = 3D/4$. The parameters that varied from one integration to another were L_x and D (i.e., L_y). In all integrations we used the value $1.6 \cdot 10^{-11}$ s^{-1} for the northward (y-) derivative of f, the Coriolis parameter.

For the first four integrations we had $L_x = 3.75 \cdot 10^6$ m and $D = 3.00 \cdot 10^6$ m. With the initial values that we have listed above and the values of L_x and D that we have just mentioned the perturbation flow will initially carry an amount of energy that is approximately 9% of the total energy.

The first case that we integrated was a linearized version of the simple model. Some of the results from this integration are shown in Figures 7.1-7.4. Figure 6.3, which is for the linear stability analysis of this case, shows that with $L_x = 3.75 \cdot 10^6$ m and $D = 3.00 \cdot 10^6$ m this type of zonal flow is stable. This is confirmed by the numerical integration, all the curves on the Figures 7.1-7.4 are either constant with time or they have a time variation which seems to be expressible by trigonometric functions; none of the curves show signs of either an exponential increase or decrease with time. The trigonometric nature of the solution is most obvious from the diagrams in Figure 7.4 where some of the results have been graphed for a longer period of time than that of the

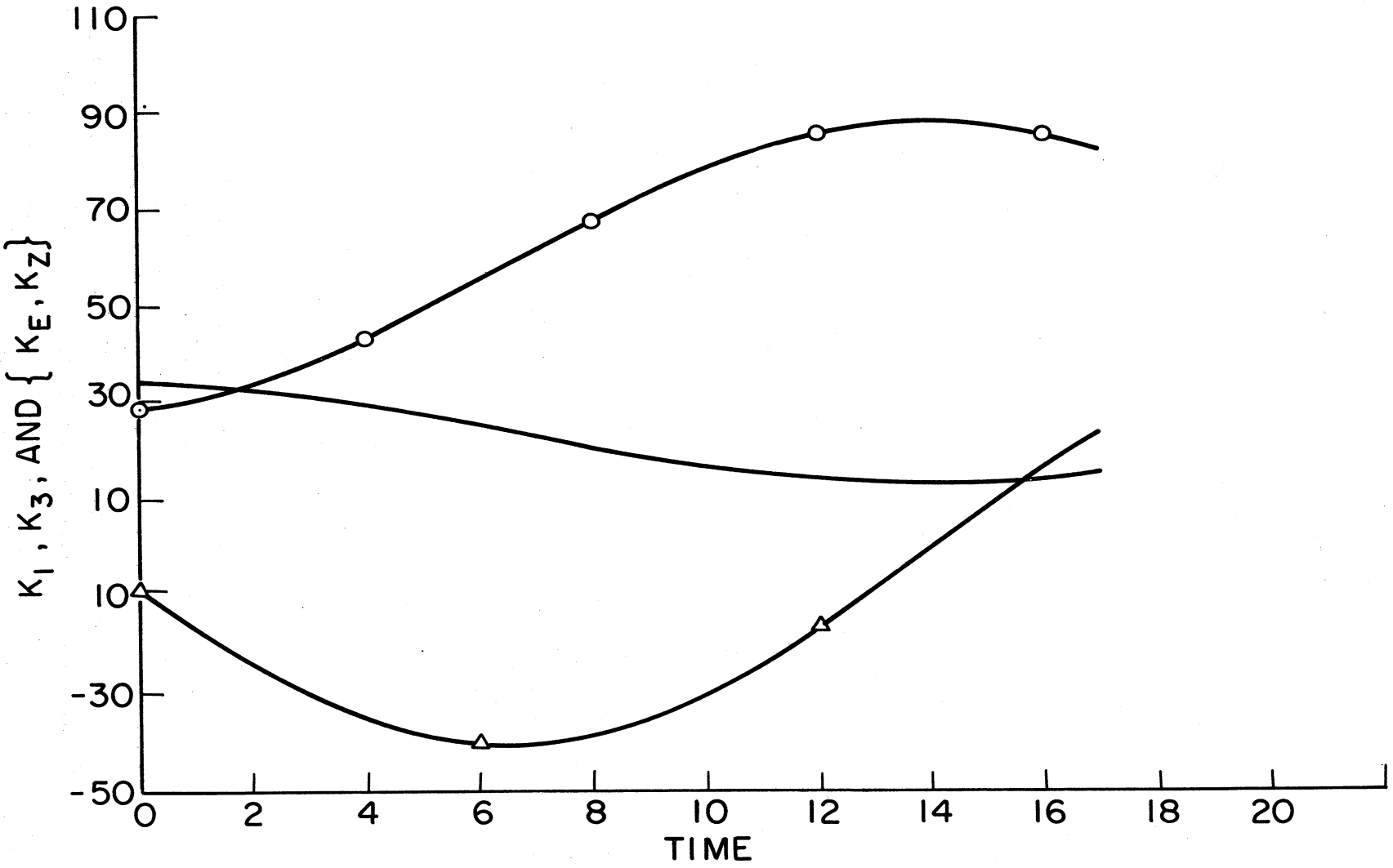

Figure 7.1. Curves showing the time variations of K_1 (solid), K_3 (with O), and $\{K_E,K_Z\}$ (with Δ). The values of $\{K_E,K_Z\}$ have all been multiplied by 10 before being graphed. K_1 and K_z are measured in m^2/s^2. $\{K_E,K_Z\}$ is measured in m^2/s^3. Time is measured in hours.

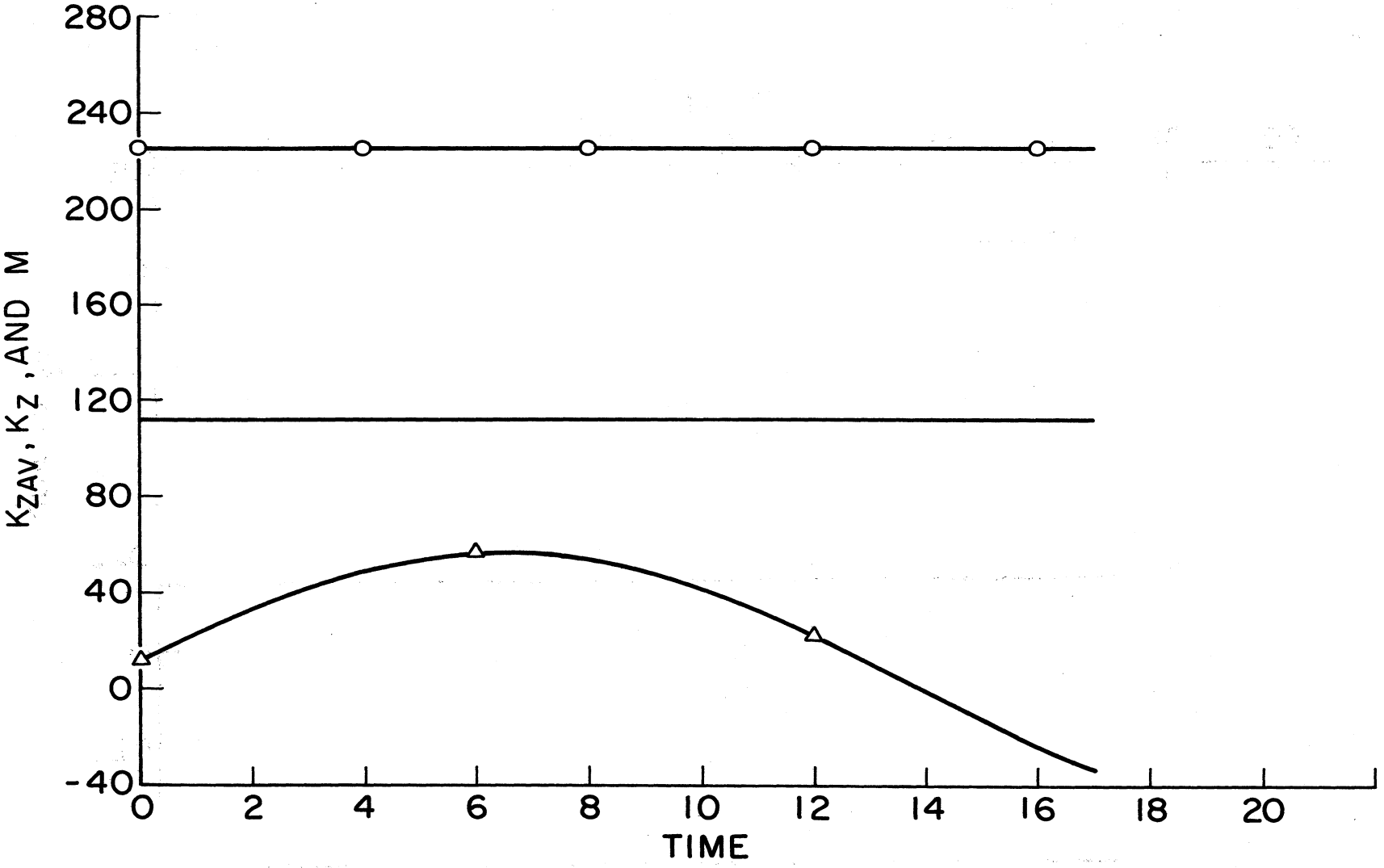

Figure 7.2. Curves showing the time variations of M (with Δ), K_{ZAV} (solid), and K_Z (with O). These are all measured in m^2/s^2. Time is measured in hours.

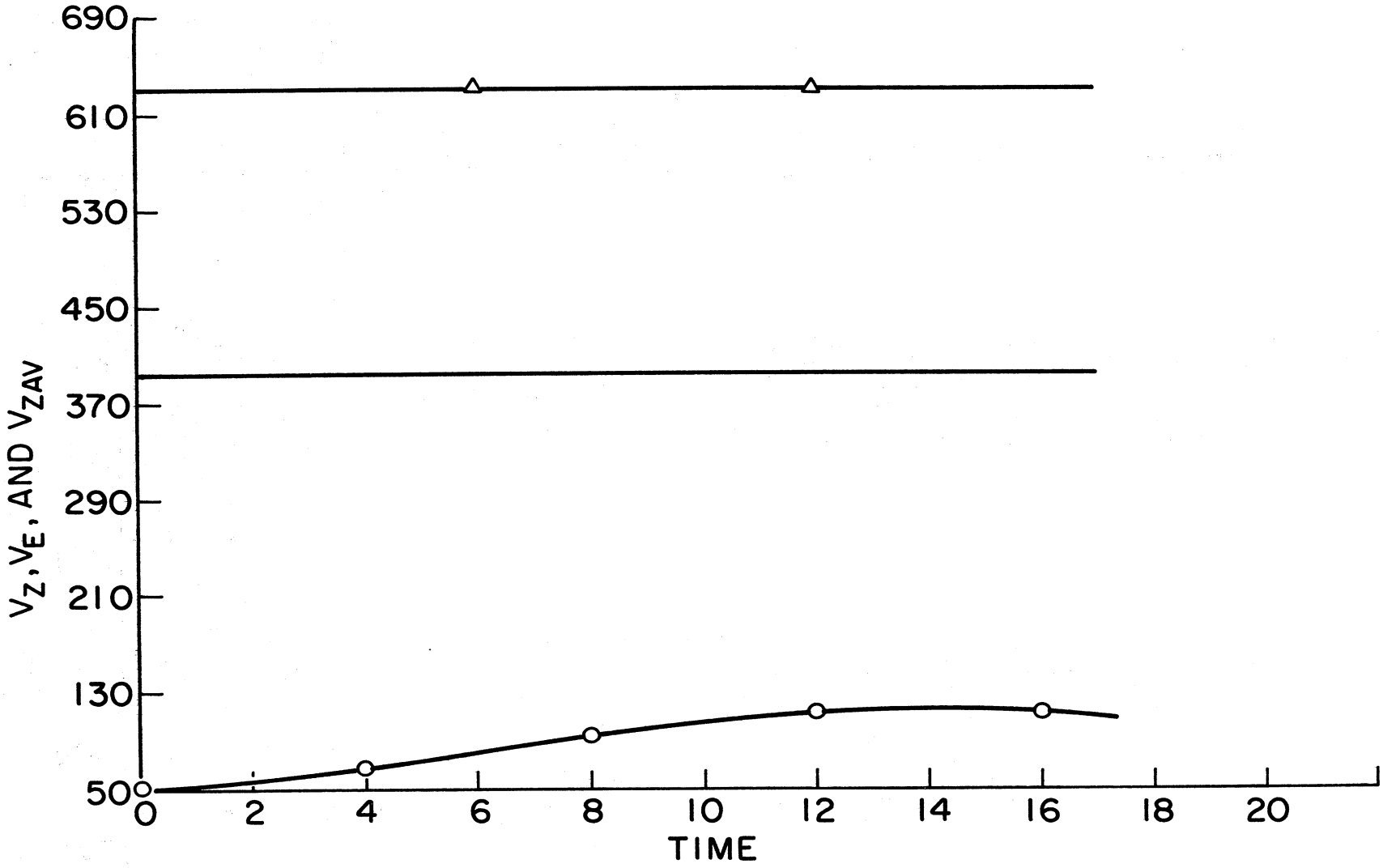

Figure 7.3. Curves showing the time variations of V_E (with O), V_Z (solid), and V_{ZAV} (with Δ). The values of all the variables have been multiplied by 10^{10} before being graphed. They are all measured in s^{-2}. Time is measured in hours.

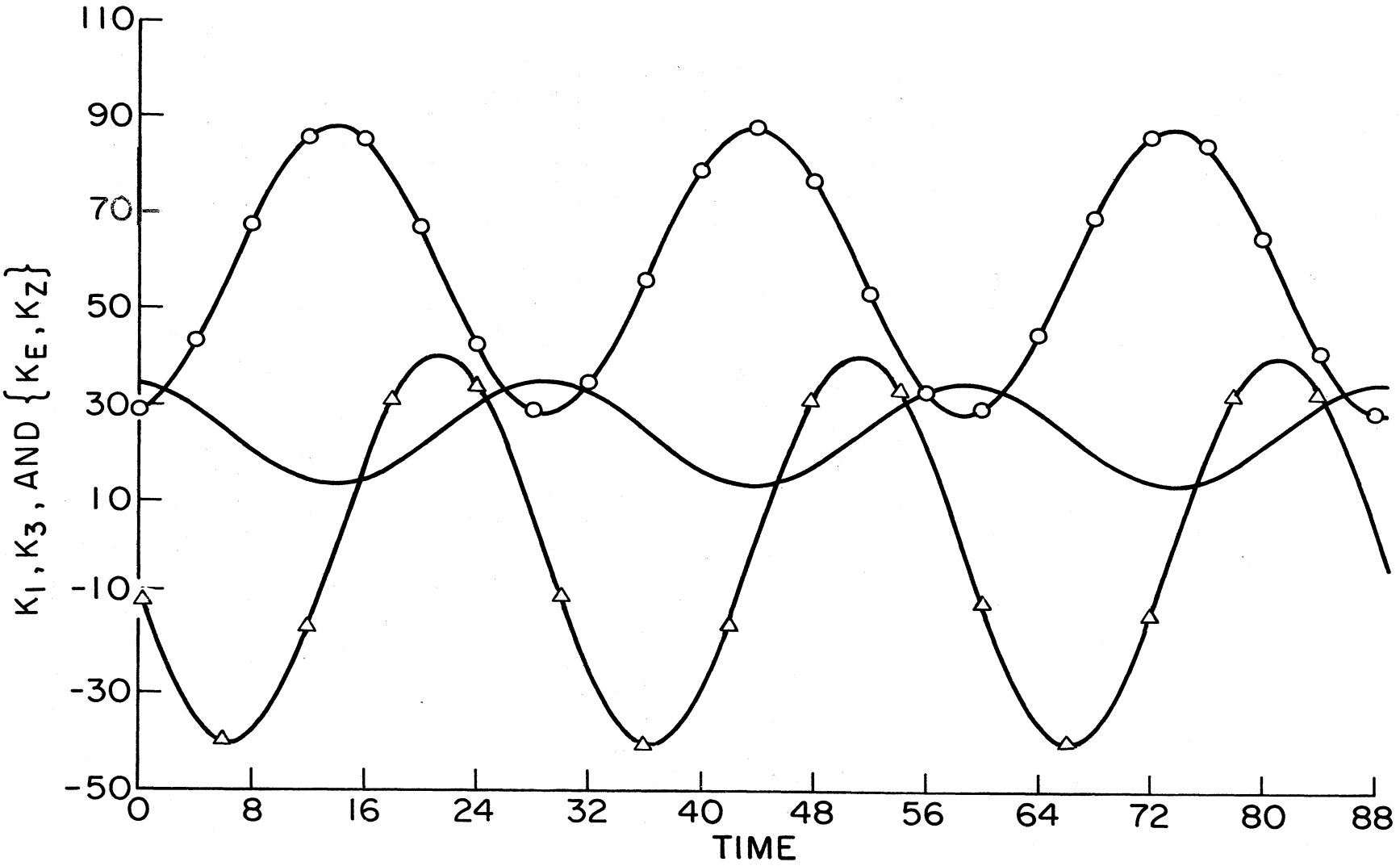

Figure 7.4. Curves showing the time variations of $\{K_E, K_Z\}$ (with Δ), K_1 (solid), and K_3 (with O). The values of $\{K_E, K_Z\}$ have all been multiplied by 10 before being graphed. K_1 and K_3 are measured in m^2/s^2. $\{K_E, K_Z\}$ is measured in m^2/s^3. Time is measured in hours.

previous figures. Figure 7.1 shows that there is a net feeding of energy into the eddy flow during the first 14 hr of the integration. It also shows that this energy is entirely used for the increase of energy on wave number 3 and that wave number 1 is giving up energy during the same period of time. At the end of this period $\{K_E,K_Z\}$ changes sign, indicating that the eddy flow is now giving up energy. Figure 7.2 shows that M varies in a directly opposite manner to $\{K_E,K_Z\}$. This is what one would expect, knowing that these quantities in this case are related to each other by the formula

$$\{K_E,K_Z\} = -QkCM,$$

and also knowing that Q, k, and C are all time independent.

Figure 7.3 shows that V_E, the eddy enstrophy, also increases during the first 14 hr. Finally, we note that K_{ZAV}, K_Z, E_Z, and V_{ZAV} are all constant with time. This is because they are all expressed in terms of B and C only, which do not change with time in this integration.

Our next case was an integration of the nonlinear equations governing the simple model. Some of the results from this integration are shown in Figures 7.5, 7.6, and 7.7. Again we notice that K_1 decreases K_3 increases to begin with; this changes when $\{K_E,K_Z\}$ changes sign, so that when the eddies are feeding the zonal flow this is done by K_3 giving up more energy than K_1 gains. Figure 7.6 shows that at any time the deviation of the zonal flow from its mean value is small. Hence, only a small fraction of the zonal kinetic energy is transformed into eddy kinetic energy. The relatively small changes of the zonal flow during the integration also manifest themselves by the close relation between the time variation of M and $\{K_E,K_Z\}$. Knowing that the zonal flow changes by only a small amount, we may expect the changes of the term B-C to be small also; hence, the time variation of $\{K_E,K_Z\}$ is mainly determined by the time variation of M.

Comparing Figures 7.7 and 7.6 we see that the variation of enstrophy is closely related to the variation of energy; when the zonal energy increases the zonal enstrophy increases, and when the zonal energy decreases this is accompanied by a decrease of zonal enstrophy. Moreover, because of this and the conservation of both total energy and total enstrophy, the changes of eddy energy and eddy enstrophy have to be related in the same way.

The first integration of the extended model was done with the zonal flow kept constant; i.e., we integrated a linearized version of the model. The results are shown in Figures 7.8-7.11. All the curves are either straight lines or they have a shape that indicates an exponential variation with time. The linear stability analysis of this case (from Figure 6.6) tells us that the zonal flow is unstable. This is confirmed by the exponential variation of the

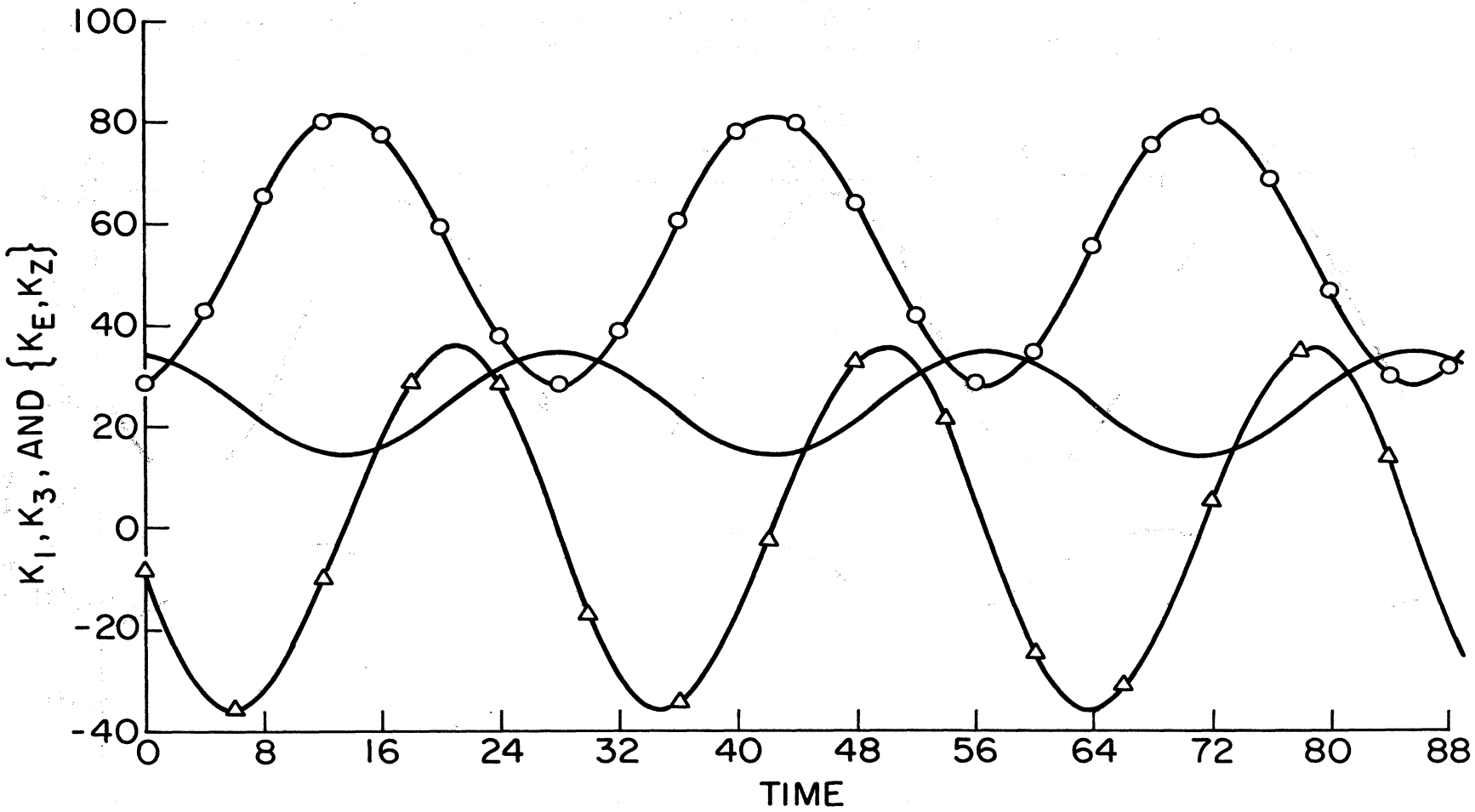

Figure 7.5. Curves showing the time variations of $\{K_E,K_Z\}$ (with Δ), K_1 (solid), and K_3 (with O). The values of $\{K_E,K_Z\}$ have all been multiplied by 10 before being graphed. K_1 and K_3 are measured in m^2/s^2. $\{K_E,K_Z\}$ is measured in m^2/s^3. Time is measured in hours.

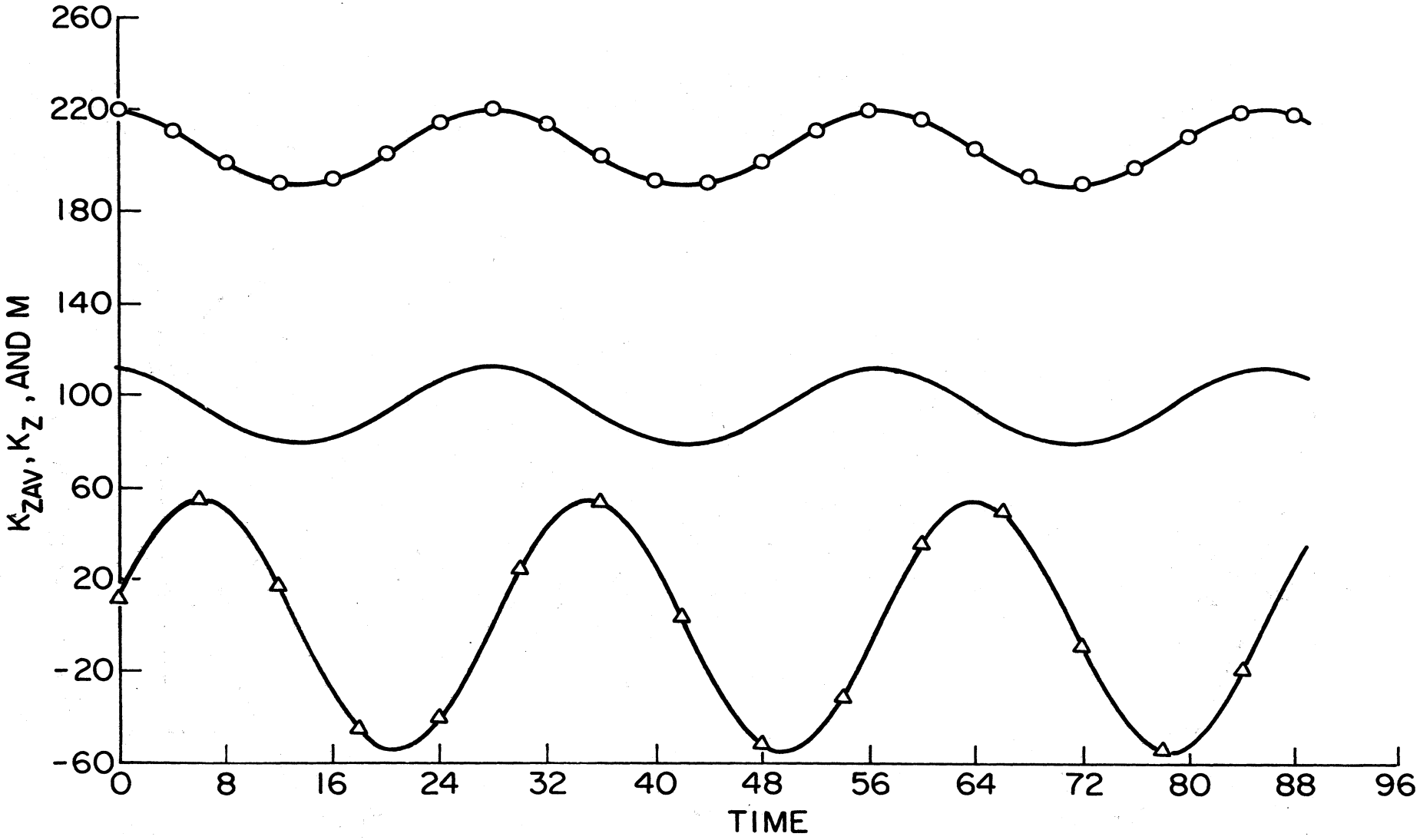

Figure 7.6. Curves showing the time variations of M (with Δ), K_{ZAV} (solid), and K_Z (with O). These are all measured in m^2/s^2. Time is measured in hours.

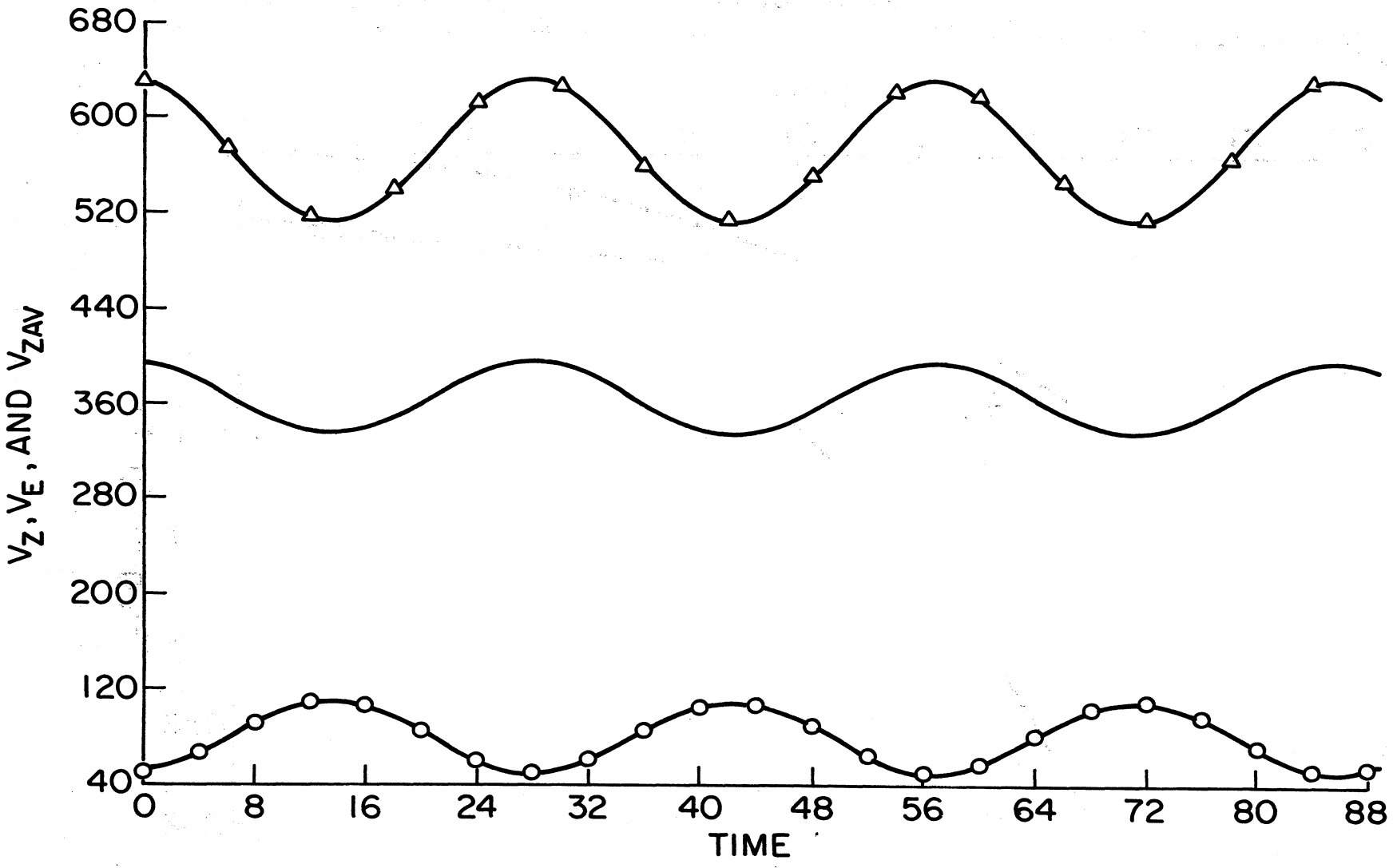

Figure 7.7. Curves showing the time variations of V_E (with O), V_Z (solid), and V_{ZAV} (with Δ). The values of all the variables have been multiplied by 10^{10} before being graphed. All variables are measured in s^{-2}. Time is measured in hours.

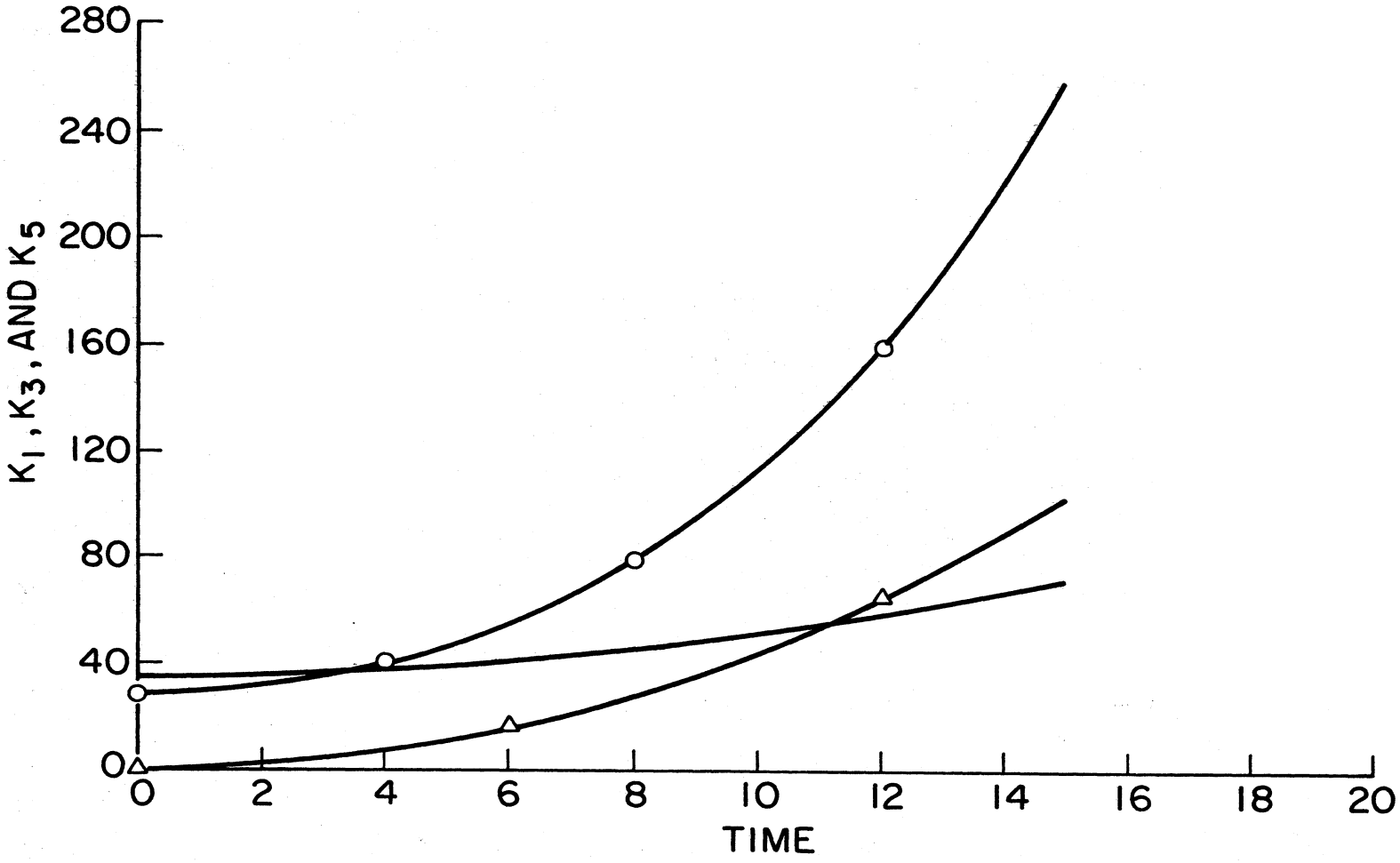

Figure 7.8. Curves showing the time variations of K_1 (solid), K_3 (with O), and K_5 (with Δ). These are all measured in m^2/s^2. Time is measured in hours.

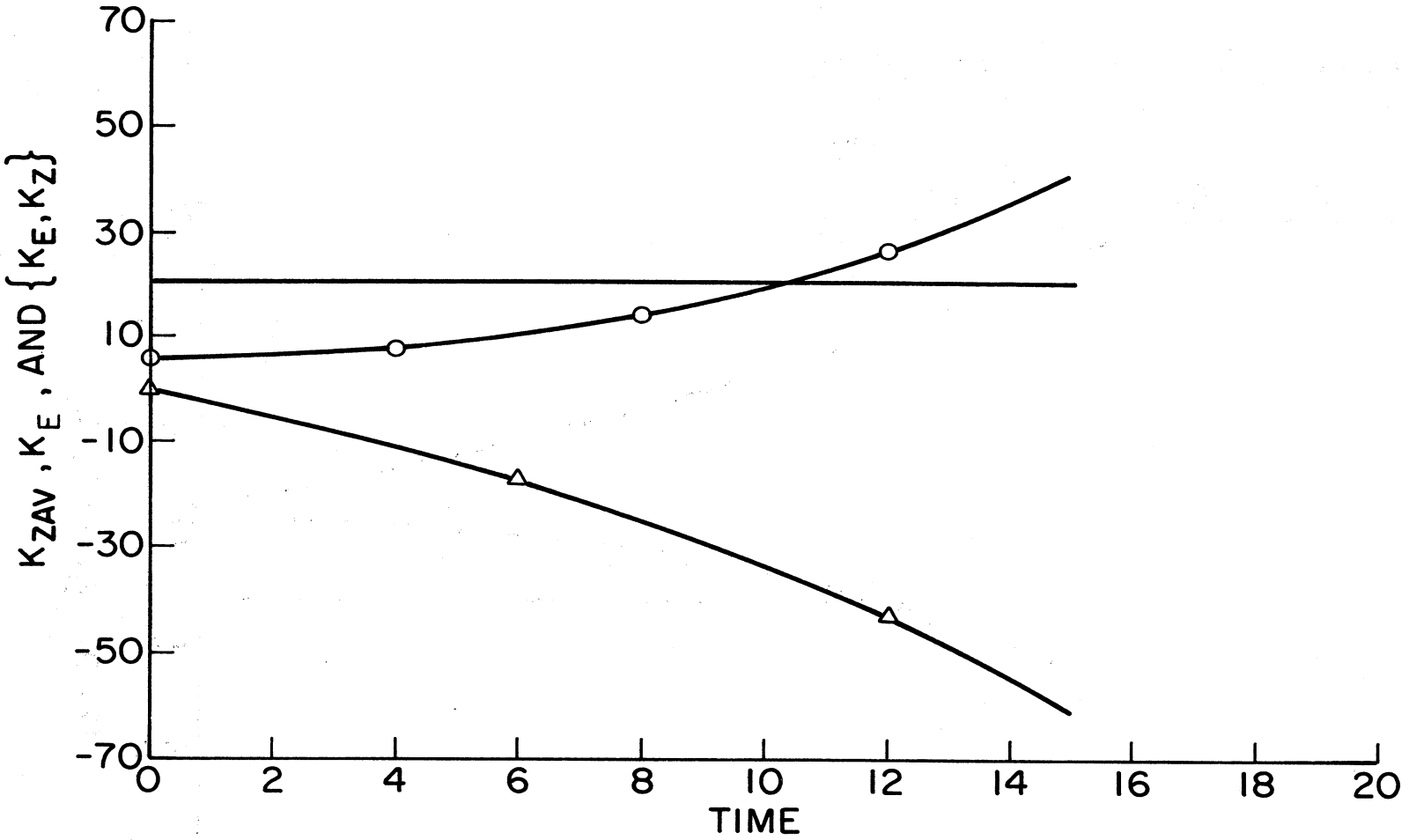

Figure 7.9. Curves showing the time variations of $\{K_E, K_Z\}$ (with Δ), K_E (with O), and K_{ZAV} (solid). The values of $\{K_E, K_Z\}$ have all been multiplied by 10 before being graphed. $\{K_E, K_Z\}$ is measured in m^2/s^3. K_E and K_{ZAV} are measured in m^2/s^2. Time is measured in hours.

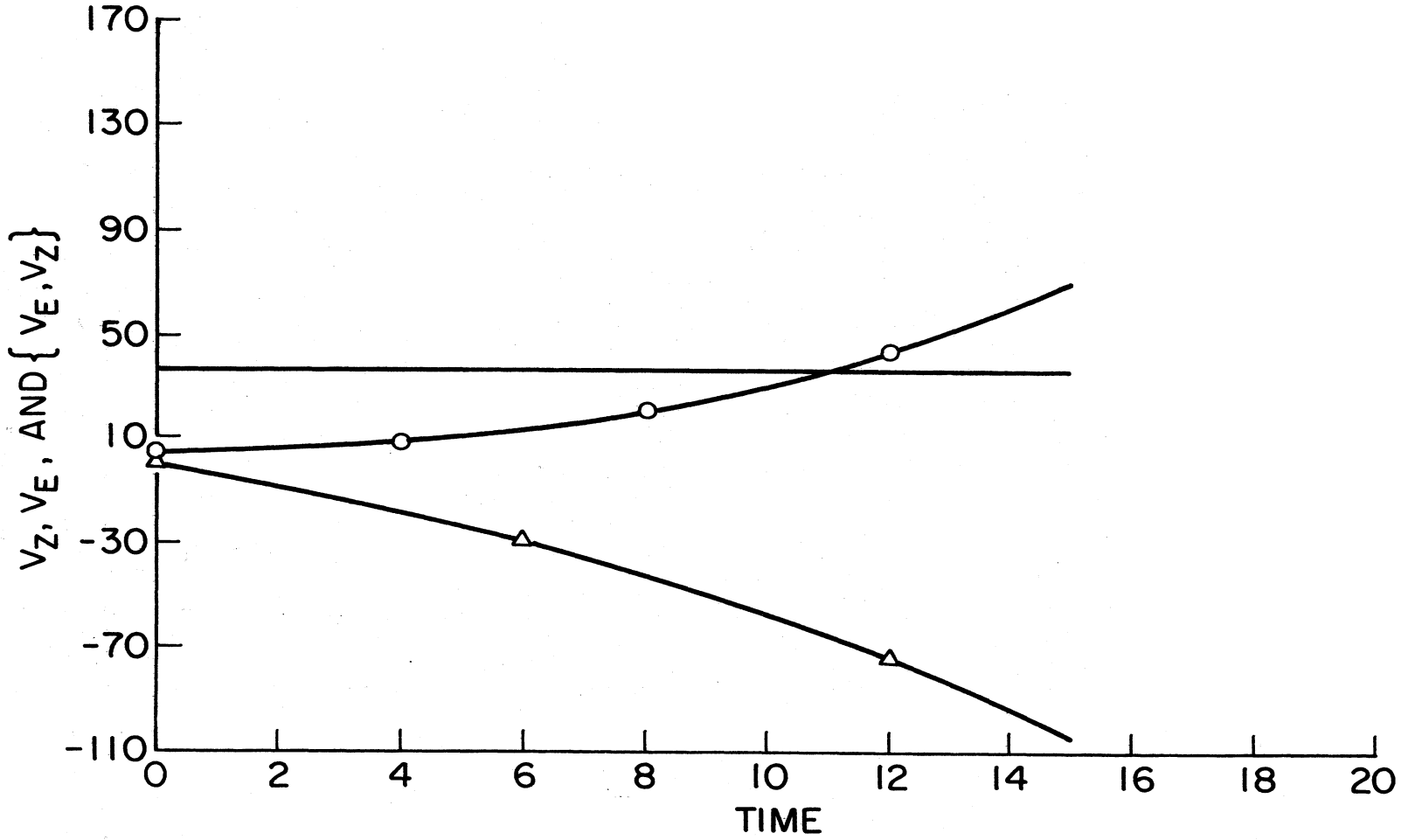

Figure 7.10. Curves showing the time variations of $\{V_E, V_Z\}$ (with Δ), V_Z (solid), and V_E (with O). The values of all the variables have been multiplied by 10^{10} before being graphed. $\{V_E, V_Z\}$ is measured in s^{-3}. V_Z and V_E are measured in s^{-2}. Time is measured in hours.

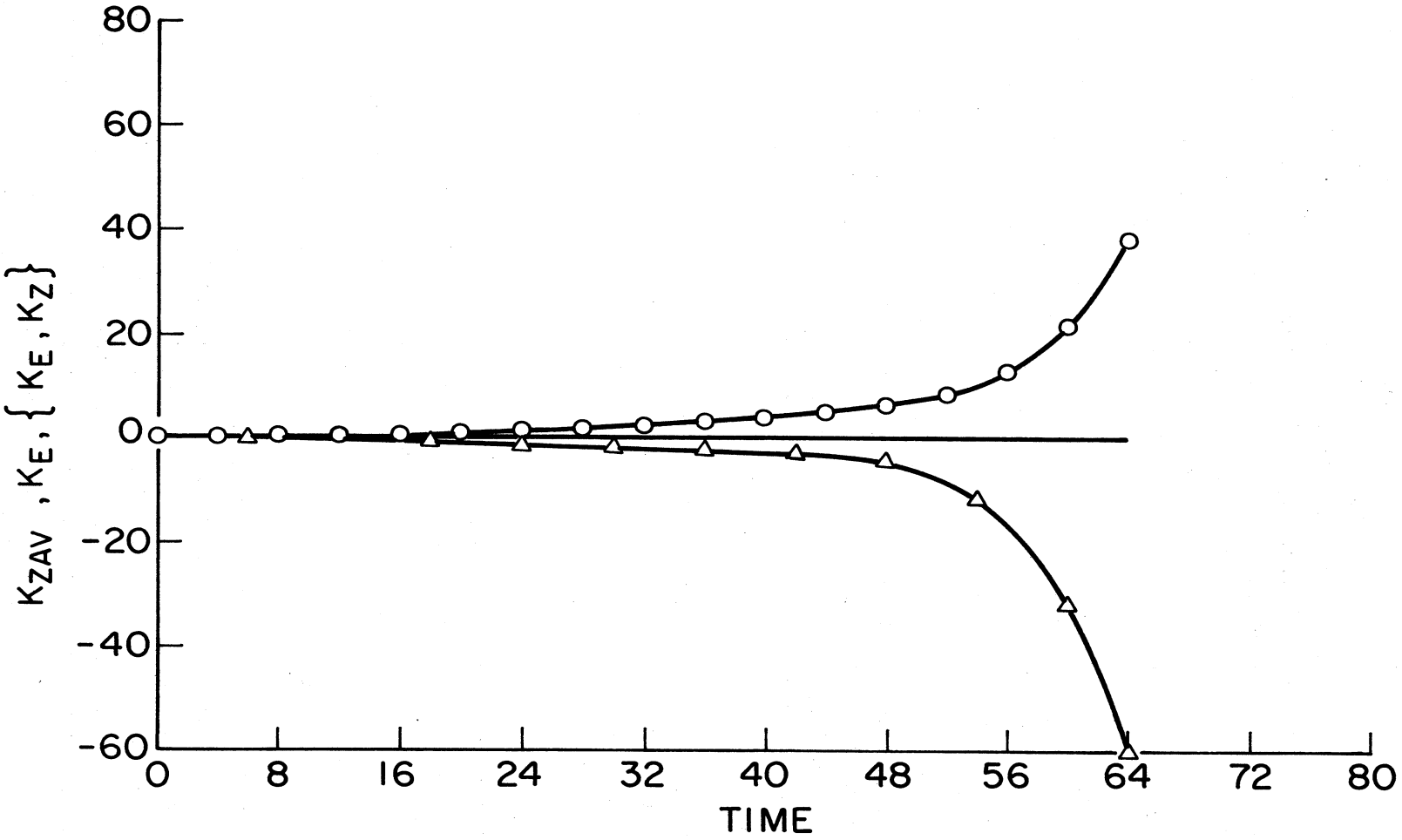

Figure 7.11. Curves showing the time variations of $\{K_E,K_Z\}$ (with Δ), K_{ZAV} (solid), and K_E (with O). The values of $\{K_E,K_Z\}$ have all been multiplied by 10 before being graphed. $\{K_E,K_Z\}$ is measured in m^2/s^3. K_{ZAV} and K_E are measured in m^2/s^2. Time is measured in hours.

quantities graphed in Figures 7.8-7.11. The first thing that we note about this integration is the steady increase of kinetic energy on all the eddy wave numbers. Of course, this implies that the total eddy kinetic energy is increasing and also that there is a steady conversion of zonal kinetic energy into eddy kinetic energy; as can be seen from Figure 7.9. Figure 7.10 also tells us the same as we learned from Figure 7.7, namely that the variation of enstrophy is related to the variation of energy. Figure 7.9 shows a steady increase of the eddy kinetic energy. Figure 7.10 shows a similar increase of the eddy enstrophy. Figure 7.11 has been added simply to show that the numerical solutions obtained for the eddy quantities are truly exponential.

The last case using the values of L_x and D that we listed to begin with, was a nonlinear integration of the extended model. Results from this integration are shown on Figures 7.12-7.14. From the linear stability analysis and from the previous integration we know that this integration is linearly unstable.

In the stable cases that we integrated with the simple model the linear and the nonlinear version behaved in a way very similar to each other. In the present unstable case we see that although there is a correspondence to begin with the two integrations become entirely different after some time. This is, of course, due to the constraints on energy and enstrophy that we have in the nonlinear case, which prevent the dependent variables from becoming unbounded.

Looking at Figure 7.12 we see that the energy is increasing on all three wave numbers to begin with. Also we notice that due to the addition of more wave numbers in the y-direction we no longer find solutions which are simple trigonometric functions of time.

Figure 7.13 shows that at the time when the eddy kinetic energy has its maximum value the zonal available energy is almost zero. Comparing these results with the results that we obtained from the integration of the simple model, we find that the variation of eddy kinetic energy and zonal available energy is much greater in the present case than it was with the simple model. This is possibly a way in which the instability that we found by the linear stability analysis manifests itself in a nonlinear integration.

So far we have found a close correspondence between the variation of energy and enstrophy. Comparing Figures 7.13 and 7.14 we find that there is a close correspondence to begin with in the present integration also, but that this similarity breaks down some time after 40 hr of integration. After that the conversions of energy and enstrophy change signs at different times and they reach their minimum values at different times. This could be due to the fact that there are more waves interacting at this later stage than during the first part of the integration. On the other hand there is a possibility that this could be due to phase errors resulting from the truncation in the time integration scheme. In addition we may note that there is also a truncation error due to the fact that we are using gridpoints in the y-direction. The

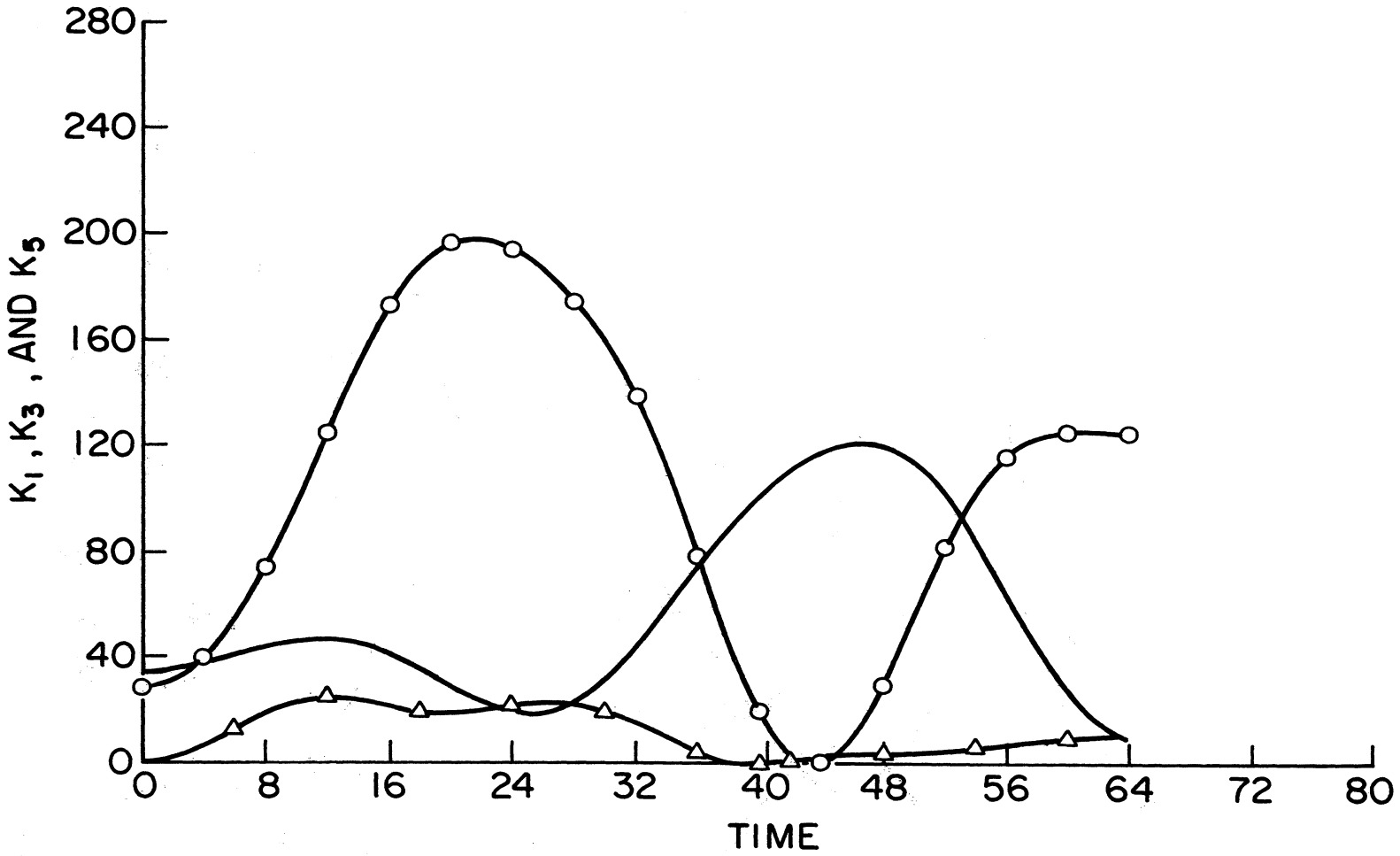

Figure 7.12. Curves showing the time variations of K_1 (solid), K_3 (with O), and K_5 (with Δ). These are all measured in m^2/s^2. Time is measured in hours.

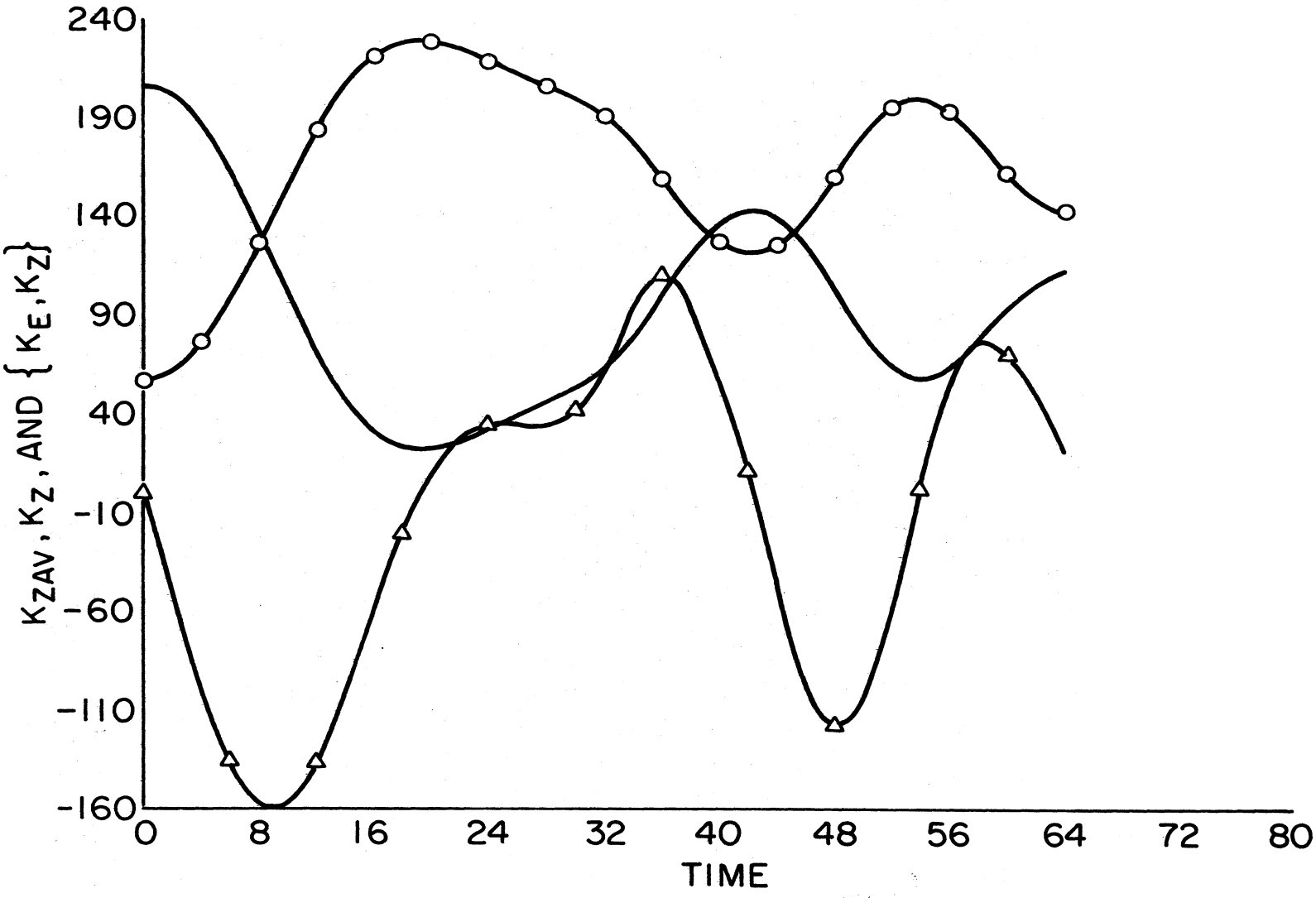

Figure 7.13. Curves showing the time variations of $\{K_E, K_Z\}$ (with Δ), K_{ZAV} (solid), and K_E (with O). The values of $\{K_E, K_Z\}$ have all been multiplied by 10 before being graphed. $\{K_E, K_Z\}$ is measured in m^2/s^3. K_E and K_{ZAV} are measured in m^2/s^2. Time is measured in hours.

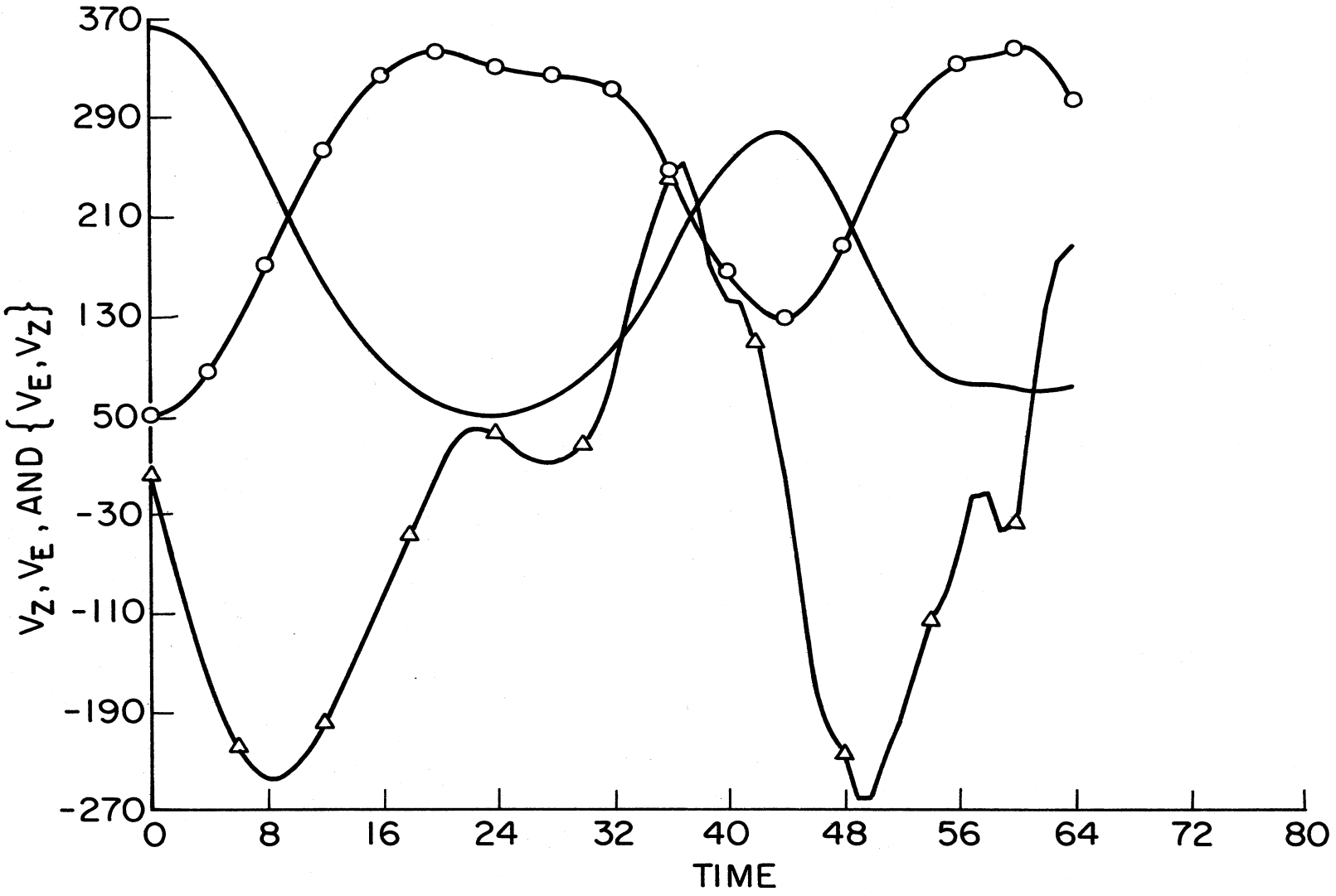

Figure 7.14. Curves showing the time variations of $\{V_E,V_Z\}$ (with Δ), V_Z (solid), and V_E (with O). The values of all the variables have been multiplied by 10^{11} before being graphed. $\{V_E,V_Z\}$ is measured in s^{-3}. V_Z and V_E are measured in s^{-2}. Time is measured in hours.

effects of time truncations have been demonstrated for a truncated spectral system by Baer and Simons (1970).

Our next case is a nonlinear integration of the simple model. For this integration we changed the zonal wave length to be $2.00 \cdot 10^6$ m. All other parameters remained the same. From the stability diagram, Figure 6.3, we see that the zonal flow for this case is dynamically unstable. Due to the $1+Q$ and $1+9Q$ coefficients in the expressions of the eddy energies the amount of eddy kinetic energy that we now have initially is slightly different from the amount we had before, when we had a different value of L_x. With the present value of L_x it is approximately 6% of the total energy.

Results from this integration are shown on Figures 7.15-7.17. Comparing these results with the results from the stable case we notice the large differences between the amplitudes in the two cases. The maximum amount of energy on wave number 3, K_3, is about twice as large in the present integration compared with the stable integration. Also we see from Figure 7.16 that in the present integration the zonal available energy gets close to zero. In the previous stable integration it never got below 80 m^2/s^2. As we also saw in all previous integrations that were linearly unstable, there is an increase of energy on all eddy wave numbers to begin with. At the time when the energy on wave number 3 reaches its maximum value the amount of energy on wave number 1 is close to zero. At the same time the zonal available energy is close to zero. This tells us that the zonal flow has given up almost all the energy it possibly can, and that this energy now is in wave number 3, only. From the diagrams we see that the maximum value of energy in wave number 3 is reached after 30 hr. At the same time $\{K_E, K_Z\}$ becomes positive, indicating that from now on and for some time energy is given up by the eddies to the zonal flow. Looking at Figure 7.16 we find that M changes sign at the same time, hence also in this unstable case we find that M is the important factor as far as the sign of the energy conversion is concerned. This is what one would expect knowing that the sign of M gives the slope of the trough and ridge lines and hence, the direction of the momentum transport. Comparing the graph of K_{ZAV} on Figure 7.16 with the graph of V_{ZAV} on Figure 7.17 we see that the enstrophy has a similar variation as the energy in this integration.

Our last case is a nonlinear integration of the extended model with the same parameter values and initial values that we have used in the previous integration of the simple model. Results from this integration are shown in Figures 7.18-7.20. The stability analysis tells us that this integration is linearly unstable. As in the previous unstable cases we have studied, we find in the present case also that there is an increase of eddy energy on all wave numbers to begin with. Comparing this integration with the previous integration of the extended model (Figures 7.12-7.14), we see that in the present case there is a much faster increase of energy on wave number 1 than what there was in the previous integration. Also the maximum value that this energy reaches early in the integration is much larger in the present case than the

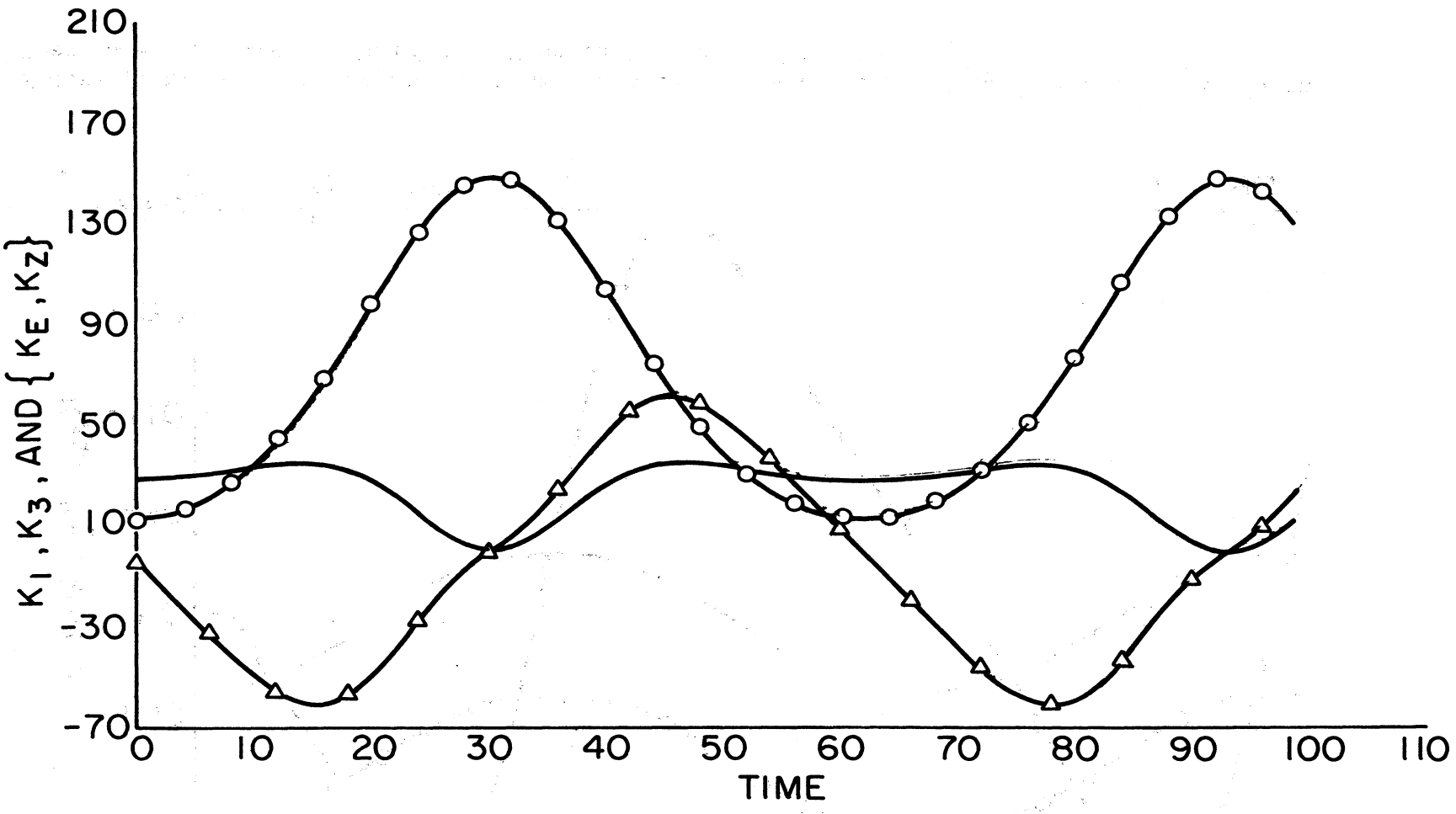

Figure 7.15. Curves showing the time variations of $\{K_E,K_Z\}$ (with Δ), K_1 (solid), and K_3 (with O). The values of $\{K_E,K_Z\}$ have all been multiplied with 10 before being graphed. $\{K_E,K_Z\}$ is measured in m^2/s^3. K_1 and K_3 are measured in m^2/s^2. Time is measured in hours.

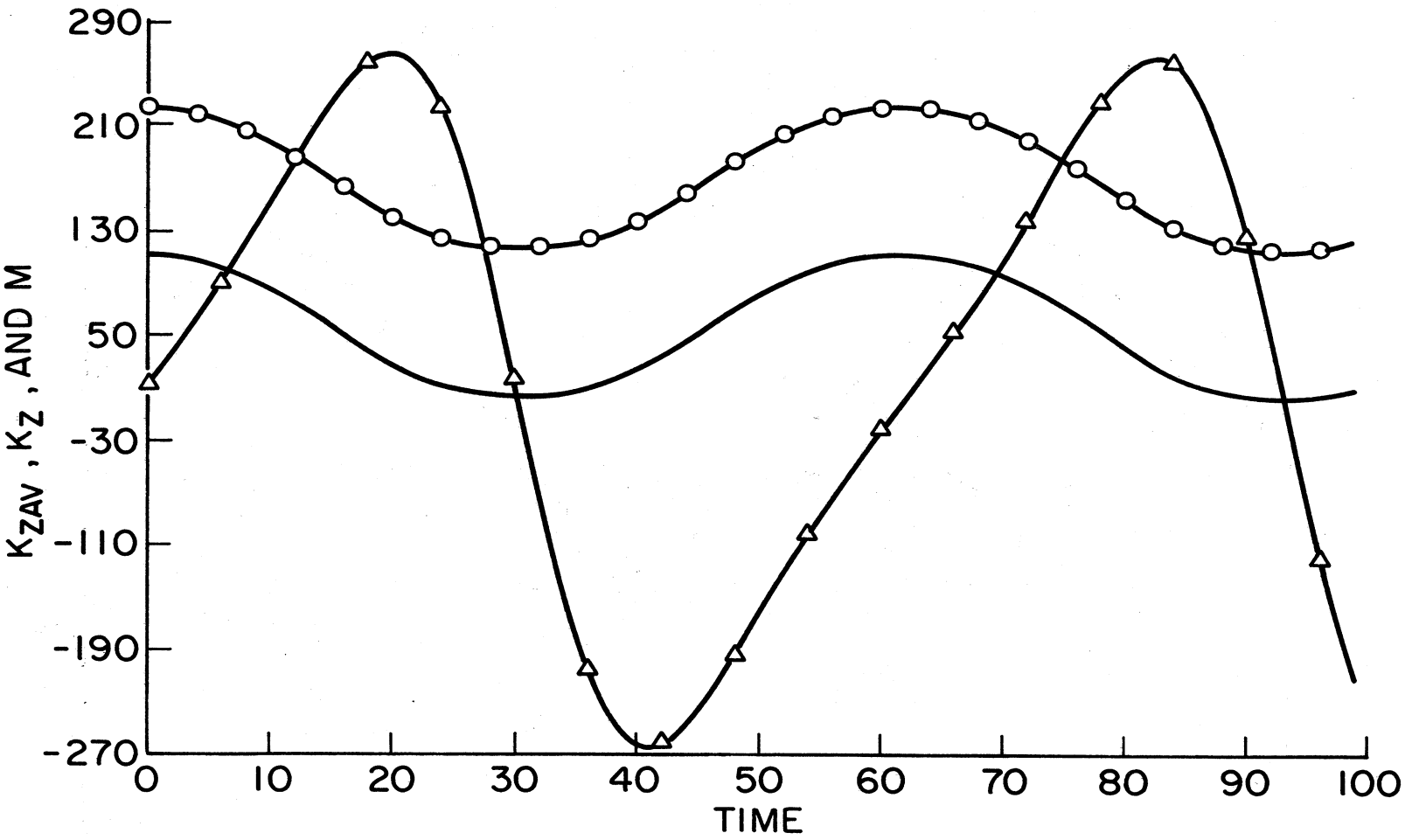

Figure 7.16. Curves showing the time variations of M (with Δ), K_{ZAV} (solid), and K_Z (with O). These are all measured in m^2/s^2. Time is measured in hours.

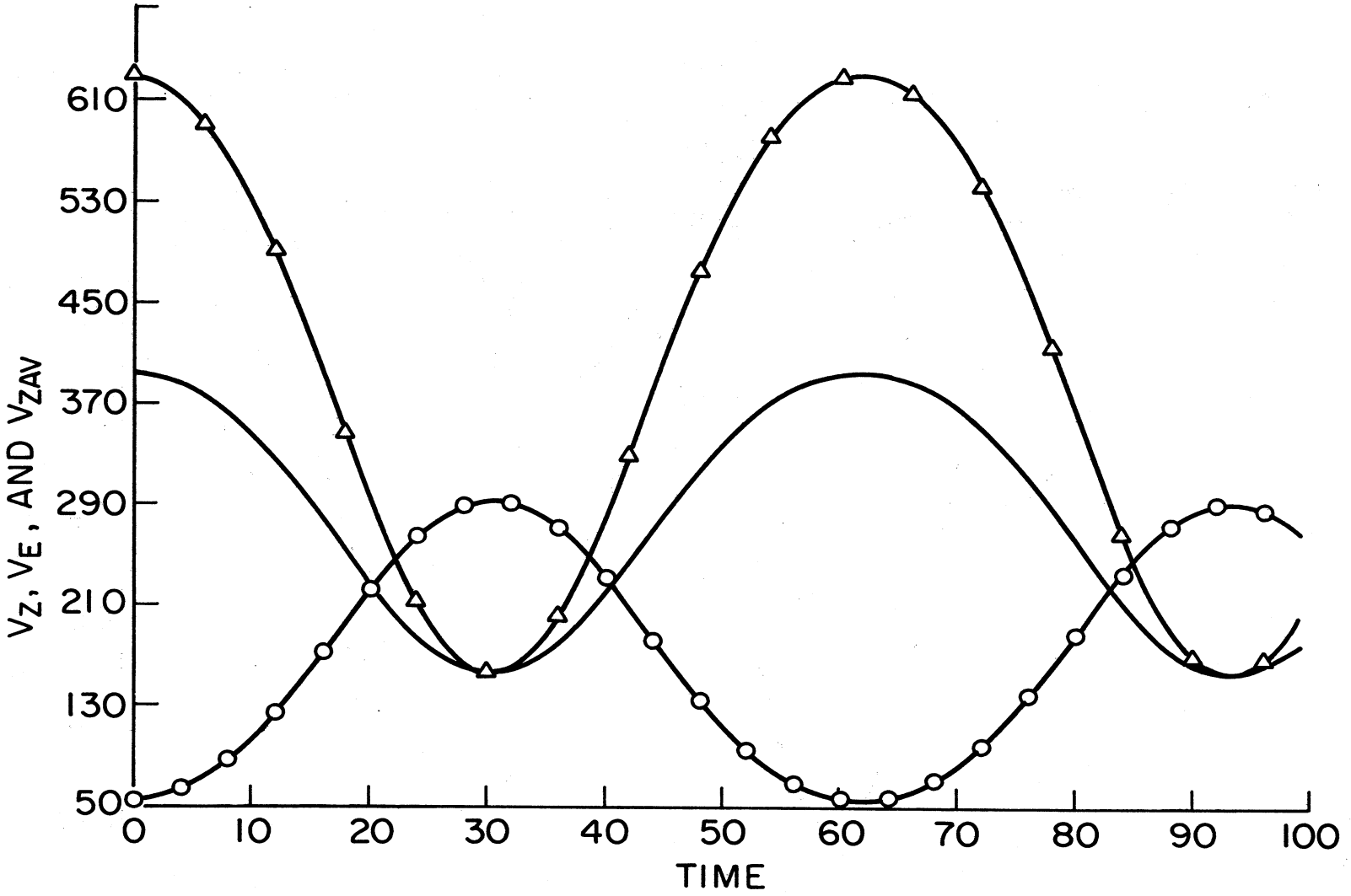

Figure 7.17. Curves showing the time variation of V_E (with O), V_Z (solid), and V_{ZAV} (with Δ). The values have been multiplied by 10^{10} before being graphed. These are all measured in s^{-2}. Time is measured in hours.

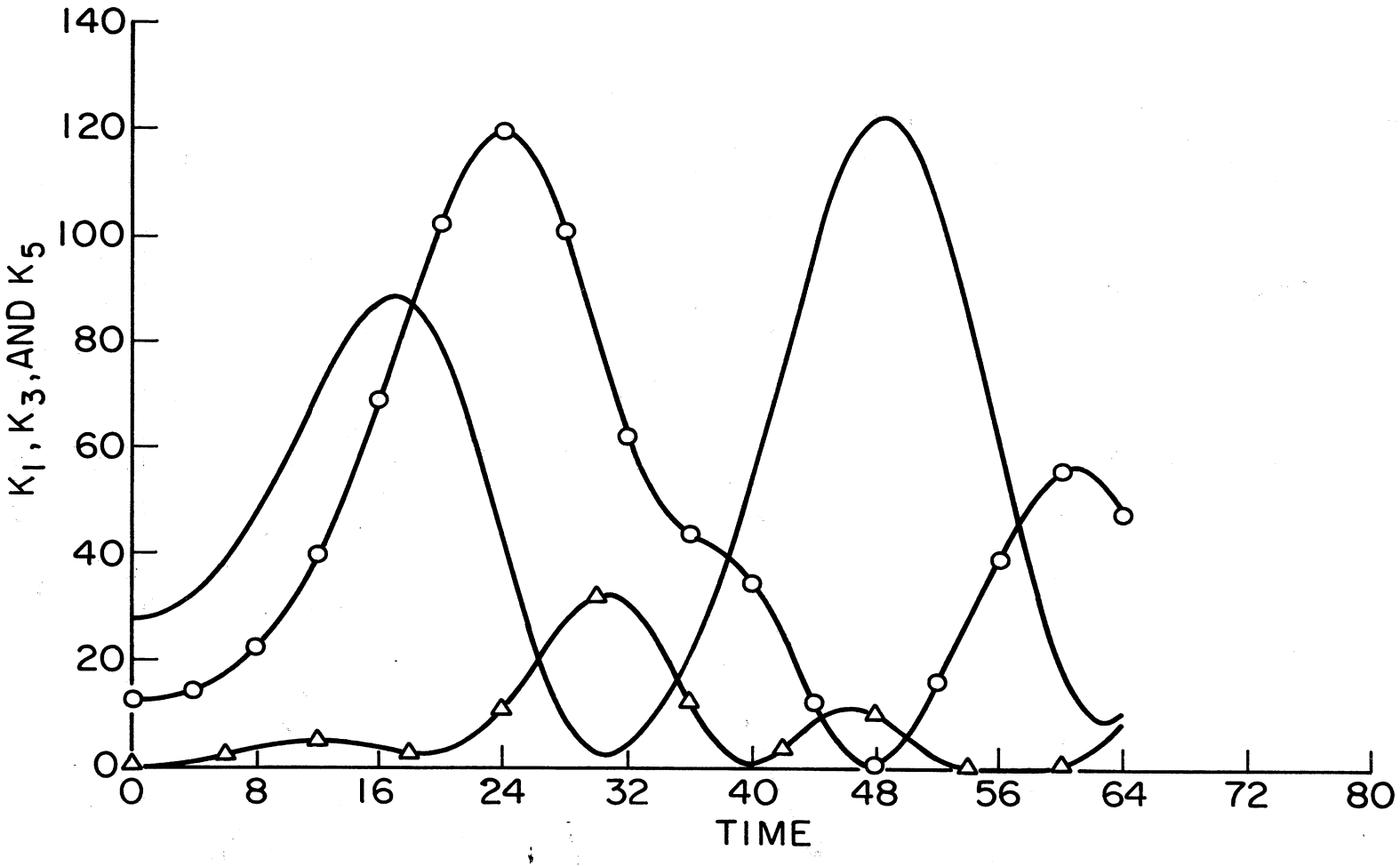

Figure 7.18. Curves showing the time variations of K_1 (solid), K_3 (with O), and K_5 (with Δ). These are all measured in m^2/s^2. Time is measured in hours.

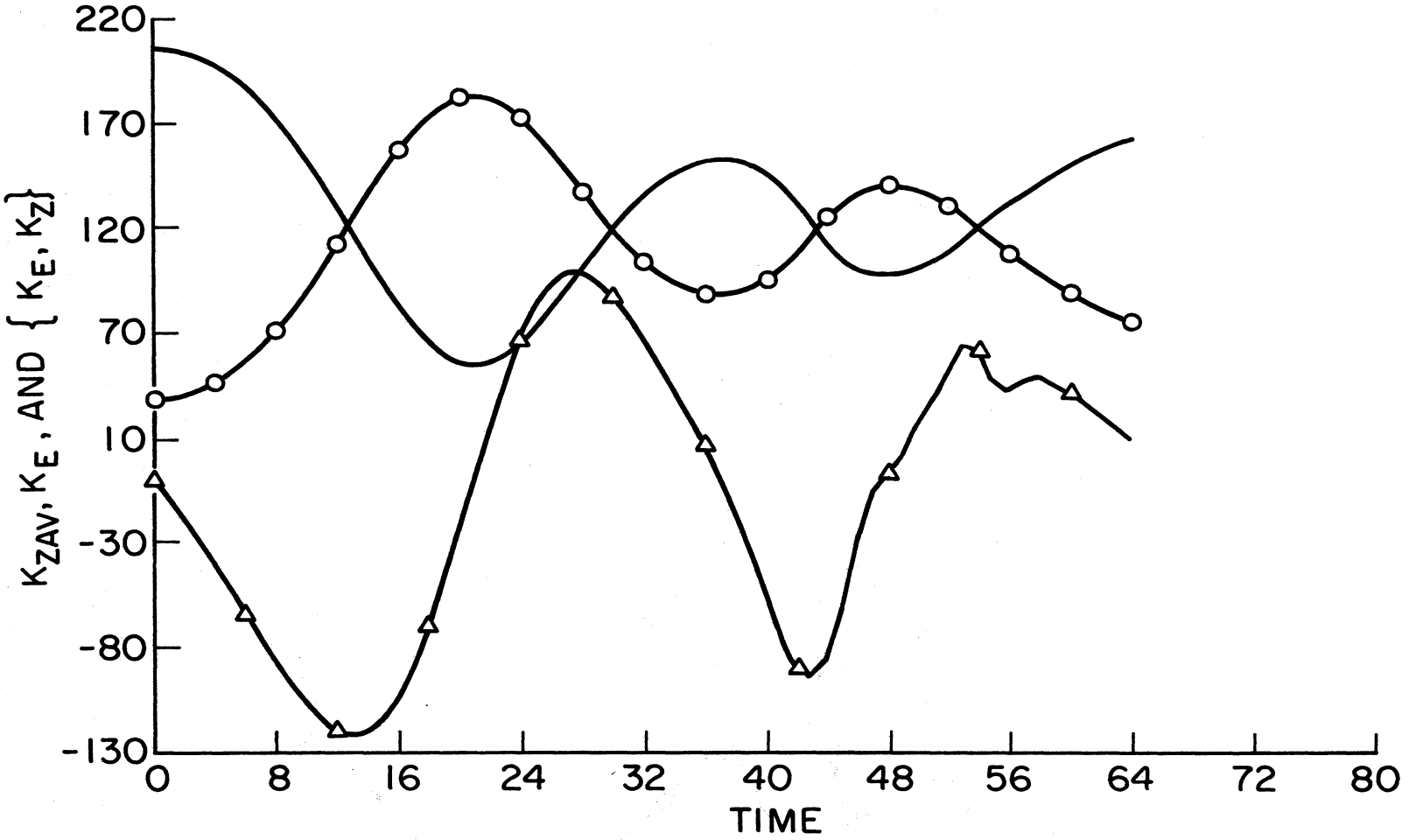

Figure 7.19. Curves showing the time variations of $\{K_E,K_Z\}$ (with Δ), K_E (with O), and K_{ZAV} (solid). The values of $\{K_E,K_Z\}$ have all been multiplied by 10 before being graphed. $\{K_E,K_Z\}$ is measured in m^2/s^3. K_E and K_{ZAV} are measured in m^2/s^2. Time is measured in hours.

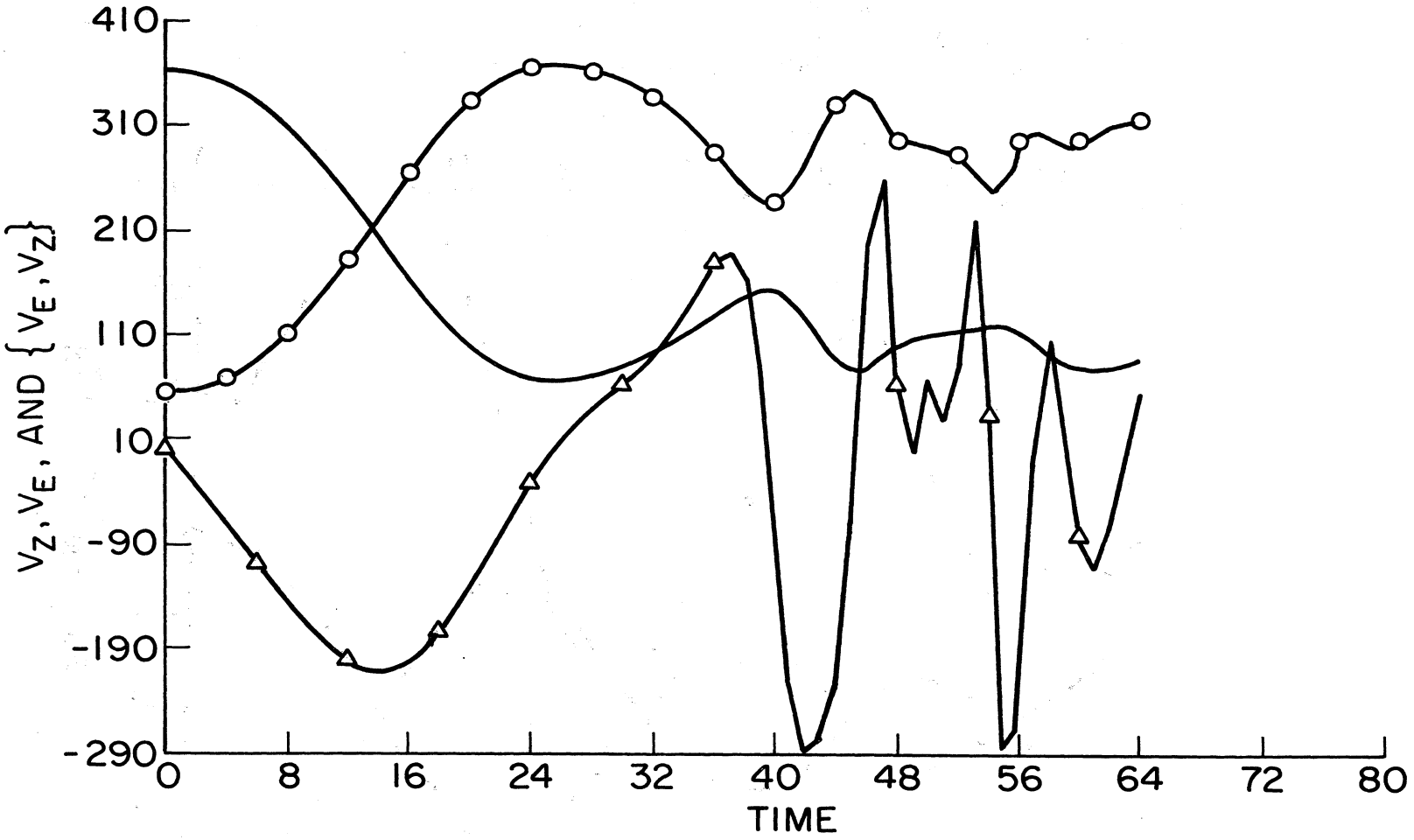

Figure 7.20. Curves showing the time variations of $\{V_E,V_Z\}$ (with Δ), V_Z (solid), and V_E (with O). The values of all the variables have been multiplied by 10^{11} before being graphed. $\{V_E,V_Z\}$ is measured in s^{-3}. V_Z and V_E are measured in s^{-2}. Time is measured in hours.

corresponding maximum value in the previous integration. In the previous unstable integration of the simple model we found that the zonal available energy became almost zero at two times during the integration. Studying the graph of K_{ZAV} on Figure 7.13 we see that here the available energy goes down to approximately 20 m^2/s^2. Later it reaches a relative minimum of approximately 60 m^2/s^2. In the present case the available energy reaches minimum values of approximately 50 m^2/s^2 and approximately 100 m^2/s^2. The only difference between the present integration and the previous simple integration is the number of wave numbers in the eddy flow. Hence, we see that this is important as to how much of the zonal energy is transformed into eddy energy. The only difference between the two nonlinear integrations of the extended model that we have performed is the zonal wave length of the eddy flow. Remembering that the amounts of zonal energy given up to the eddies were different in the two cases we realize that the wave length of the eddy flow is important for the amount of energy that is given up to the eddies. Finally, imagine that we made an integration of the extended model with the same zonal wave length and the same width of the channel as we are presently using, and with the values of the dependent variables at 40 hr in the present integration as initial values; then we would get a minimum of the zonal available energy having the same minimum value of this energy as the minimum at 47-48 hr in the last integration that we are now studying. The minimum values of the zonal available energy at this minimum point and at the minimum point at 17-18 hr are different. This is because the "initial" values are different; the shape of the zonal flow, the eddy kinetic energy, and also the distribution of energy among the different waves of the eddy flow are all different at the two times. Hence, we see that the maximum amount of zonal energy that is transformed into eddy kinetic energy depends on what conditions the flow starts from.

Comparing the graphs on Figure 7.20 with those on Figure 7.19 we find, as we found in the previous integration of the extended model, that the energy and enstrophy has a variation which is very similar in the beginning and that this similarity breaks down towards the end of the integration.

CONCLUSIONS

In this report we have studied the nonlinear exchanges of energy and enstrophy between the zonal flow and a disturbance. Both the zonal wave length and the number of waves in the disturbance have been allowed to vary. The study shows that the transfer of energy and enstrophy between the zonal flow and the disturbance depends on both of these parameters. Also, we found that they depend on the fraction of the total energy that initially is in the eddies. This is in accordance with the conclusion arrived at by Platzman (1952), namely that: "the form as well as the wave length, of the disturbance is a controlling factor in determining the initial energy transfer, and that conclusive inferences cannot be made merely from the character of the mean flow."

By a linear stability analysis we found that a given zonal wind profile may be stable for a disturbance which is made up from two wave numbers in the y-direction and unstable if we add one more wave number in this direction. When we compared the results from the linear stability analysis of the different cases with the magnitudes of the two-dimensional wave numbers in these cases, we found that the question of stability or instability of the zonal flow seems to be related to how the energy cascades when it is given up by the zonal flow.

REFERENCES

Baer, F., 1970a: Analytical Solutions to Low-Order Spectral Systems, Arch. Met. Geoph. Biokl., Ser. A, 19, pp. 255-282.

Baer, F., 1970b: Dependence of the Highly Truncated Spectral Vorticity Equation on Initial Conditions, J. Atmos. Sci., Vol. 27, pp. 987-999.

Baer, F., 1971: Energetics of Low-Order Spectral Systems, Tellus, Vol. 23, pp. 218-231.

Baer, F. and T. J. Simons, 1970: Computational Stability and Time Truncation of Coupled Nonlinear Equations with Exact Solutions, Mon. Wea. Rev., Vol. 98, pp. 665-679.

Charney, J. G., 1966: Some Remaining Problems in Numerical Weather Predictions, 1965-66 Seminar Series by The Travelers Research Center, Inc., pp. 61-70.

Charney, J. G. and M. E. Stern, 1962: On the Stability of Internal Baroclinic Jets in a Rotating Atmosphere, J. Atmos. Sci., Vol. 19, pp. 159-172.

Fjørtoft, R., 1953: On the Changes in the Spectral Distribution of Kinetic Energy for Two-Dimensional, Nondivergent Flow, Tellus, Vol. 5, pp. 225-230.

Lorenz, E. N., 1960: Maximum Simplification of the Dynamic Equations, Tellus, Vol. 12, pp. 243-254.

Platzman, G. W., 1952: The Increase or Decrease of Mean-Flow Energy in Large-Scale Horizontal Flow in the Atmosphere, J. Meteor., Vol. 9, pp. 347-358.

Platzman, G. W., 1964: An Exact Integral of Complete Spectral Equations for Unsteady One-Dimensional Flow, Tellus, Vol. 16, pp. 422-431.

Steinverg, H. L., 1971: On Power Laws and Nonlinear Cascades in Large Scale Atmospheric Flow, The University of Michigan, Technical Report 002630-4-T, pp. 1-143.

Wiin-Nielsen, A. C., 1961: On Short- and Long-Term Variations in Quasi-Barotropic flow, Mon. Wea. Rev., Vol. 89, pp. 461-476.

Yang, C. H., 1967: Nonlinear Aspects of the Large-Scale Motion in the Atmosphere, The University of Michigan, Technical Report 08759-1-T, pp. 1-173.